NSEL Report Series
Report No. NSEL-046
December 2016

Structural and Geotechnical Observations after the April 25, 2015 M7.8 Gorkha, Nepal Earthquake and its Aftershocks

Larry A. Fahnestock
and
Youssef M. A. Hashash

NSEL
NEWMARK STRUCTURAL ENGINEERING LABORATORY

Department of Civil and Environmental Engineering
University of Illinois at Urbana-Champaign

UILU-ENG-2016-1801

ISSN: 1940-9826

The Newmark Structural Engineering Laboratory (NSEL) of the Department of Civil and Environmental Engineering at the University of Illinois at Urbana-Champaign has a long history of excellence in research and education that has contributed greatly to the state-of-the-art in civil engineering. Completed in 1967 and extended in 1971, the structural testing area of the laboratory has a versatile strong-floor/wall and a three-story clear height that can be used to carry out a wide range of tests of building materials, models, and structural systems. The laboratory is named for Dr. Nathan M. Newmark, an internationally known educator and engineer, who was the Head of the Department of Civil Engineering at the University of Illinois [1956-73] and the Chair of the Digital Computing Laboratory [1947-57]. He developed simple, yet powerful and widely used, methods for analyzing complex structures and assemblages subjected to a variety of static, dynamic, blast, and earthquake loadings. Dr. Newmark received numerous honors and awards for his achievements, including the prestigious National Medal of Science awarded in 1968 by President Lyndon B. Johnson. He was also one of the founding members of the National Academy of Engineering.

Contact:
Prof. B.F. Spencer, Jr.
Director, Newmark Structural Engineering Laboratory
2213 NCEL, MC-250
205 North Mathews Ave.
Urbana, IL 61801
Telephone (217) 333-8630
E-mail: bfs@illinois.edu

This work was supported in part by a CEE Rapid Response Grant from the Department of Civil and Environmental Engineering at the University of Illinois at Urbana-Champaign. Partial support for Youssef Hashash from the GEER Association is gratefully acknowledged. University of Illinois CEE graduate students, Sital Uprety and Sachindra Dahal were instrumental in coordinating field reconnaissance activities, and their dedication and assistance are greatly appreciated. University of Illinois CEE undergraduate students Jiaxin Xu and Damilola Taiwo, who were supported through the CEE REU Program, provided assistance with data processing and report preparation.

The cover photographs are used with permission. The Trans-Alaska Pipeline photograph was provided by Terra Galleria Photography (http://www.terragalleria.com/).

ABSTRACT

The April 25, 2015 Gorkha (Nepal) Earthquake (M7.8) and its related aftershocks had a devastating impact on Nepal. The earthquake sequence resulted in nearly 9,000 deaths, tens of thousands of injuries, and left hundreds of thousands of inhabitants homeless. With economic losses estimated at several billion US dollars, the financial impact to Nepal is severe and the rebuilding phase will likely span many years. To investigate the effects of this event, the University of Illinois at Urbana-Champaign Department of Civil and Environmental Engineering (CEE) sponsored a team to visit Nepal, funded by a CEE Rapid Response Grant. From May 22-28, 2015, Youssef Hashash visited Nepal, in collaboration with a Geotechnical Extreme Events Reconnaissance (GEER) Association team, and collected data primarily related to geotechnical response. From June 7-13, 2015, Larry Fahnestock visited Nepal and collected data related to structural response of buildings, with focus on reinforced concrete frame structures. This report briefly summarizes geotechnical aspects of the events, which are documented more extensively in a GEER Association report, and thoroughly summarizes structural observations.

CONTENTS

Page

1 INTRODUCTION 1
2 GEOTECHNICAL ASPECTS 3
2.1 Regional tectonics 3
2.2 Earthquake setting 3
2.3 Ground response 4
2.4 Slope stability and landslides 6
2.5 Liquefaction and cyclic soil failure 10
2.6 Performance of dams and hydropower facilities 13
3 STRUCTURAL RESPONSE OF BUILDINGS 15
3.1 Low-rise to mid-rise reinforced concrete frame buildings 15
3.1.1 Common residential / commercial buildings 15
3.1.2 Developed residential / commercial buildings 21
3.1.3 Institutional buildings 25
3.2 Mid-rise to high-rise reinforced concrete frame buildings 32
4 SUMMARY 46
4.1 Geotechnical aspects 46
4.2 Structural response of buildings 46
5 REFERENCES 48
6 APPENDIX A: GPS COORDINATES FOR STRUCTURAL PHOTOGRAPHS 49

INTRODUCTION

Following the April 25, 2015 M7.8 earthquake in Nepal, the University of Illinois at Urbana-Champaign (UIUC) Department of Civil and Environmental Engineering (CEE) awarded a CEE Rapid Response Grant that supported Youssef Hashash and Larry Fahnestock to visit Nepal and investigate the effects of this event. Hashash, who was assisted by UIUC graduate students Sital Uprety and Sachindra Dahal and was co-affiliated with the Geotechnical Extreme Events Reconnaissance (GEER) Association, was on-site in Nepal from May 22-28, 2015. Fahnestock was also assisted by Uprety and Dahal and was on-site in Nepal from June 7-13, 2015.

Hashash led GEER Team B, which conducted both ground and aerial (helicopter) reconnaissance in Kathmandu and in a broad region outside the capital city, including remote regions where significant landslides occurred. Regional track logs for GEER Team B are shown in Figure 1.1 (Hashash et al. 2015). GEER observations and data collection focused on issues such as: spatial patterns of the ground shaking intensity due to the underlying rupture dynamics; seismic induced landslides, rockfalls, slumps, avalanches, slide-dams; absence/presence of surface fault ruptures; site response effects including basin edge effects and topographic effects; damage to infrastructure such as highways, bridges, dams, roads, pipelines, tunnels, and hydro-facilities; effects due to liquefaction and other ground failure mechanisms; foundation damage and how that related to structural damage (Hashash et al. 2015). Fahnestock conducted ground reconnaissance in Kathmandu and in the close surrounding area, with regional track logs shown in Figure 1.2, and focused on structural and non-structural damage to buildings.

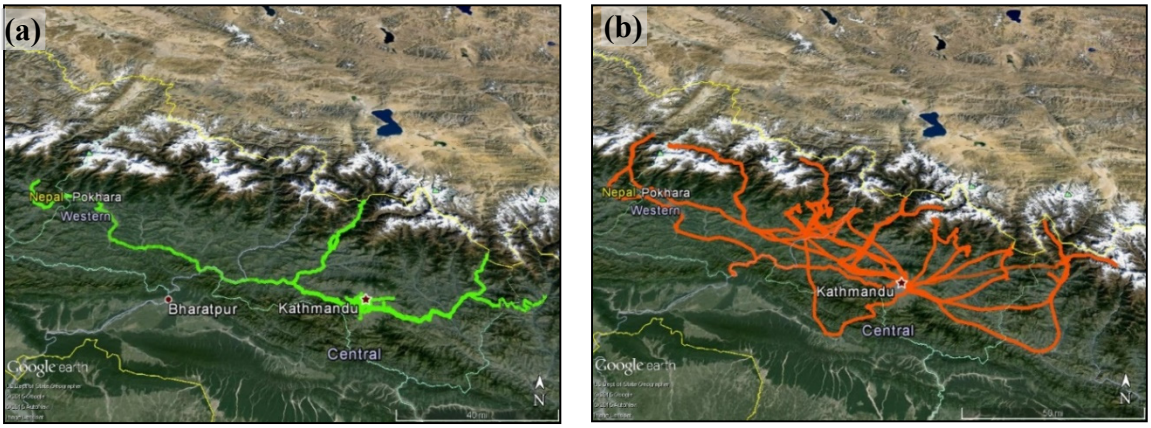

Figure 1.1 Regional track logs for GEER Team B: (a) ground reconnaissance tracks; (b) helicopter reconnaissance tracks (after Hashash et al. 2015).

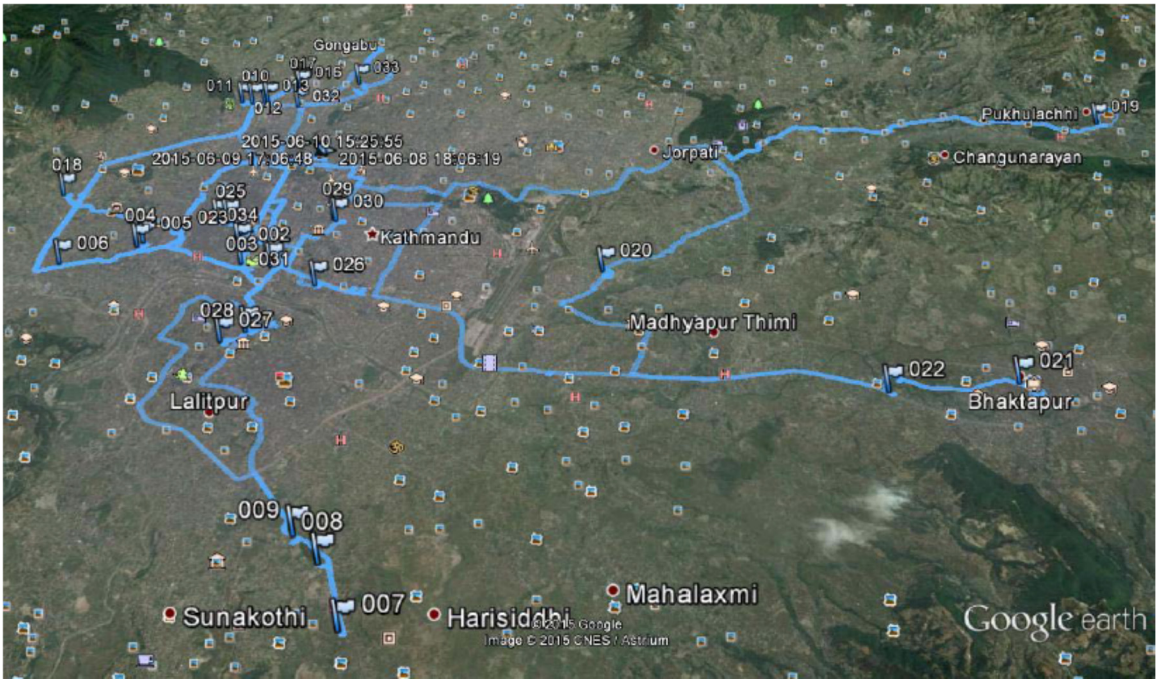

Figure 1.2 Regional track logs for Fahnestock ground reconnaissance.

This report is organized as follows. Chapter 2 summarizes geotechnical aspects of the events. Expanded coverage of the topics for Chapters 2 is contained in GEER Association Report No. GEER-040 (Hashash et al. 2015). Chapter 3 provides field observations on performance of building structures. Chapter 4 provides a summary and conclusions.

GEOTECHNICAL ASPECTS

A detailed description of the geotechnical aspects of the Nepal earthquake can be found in GEER Association Report No. GEER-040 (Hashash et al. 2015).

2.1 Regional tectonics

The April 25, 2015 M7.8 Gorkha earthquake occurred in the actively deforming central Himalayan mountain range area approximately 80 km northwest of Kathmandu, Nepal. The Himalaya is the result of the collision of the India and the Eurasia/Tibetan plate. The main Himalayan thrust (MHT) has a flat-ramp-flat geometry, where the lower flat is creeping, the upper flat is locked and the ramp itself is a transition zone (Figure 2.1). The April 25, 2015, M7.8 Gorkha earthquake as well as the May 12, 2015, M7.3 aftershock, fall into the category of Himalayan earthquakes that are large but blind as they do not rupture the surface (Figure 2.1).

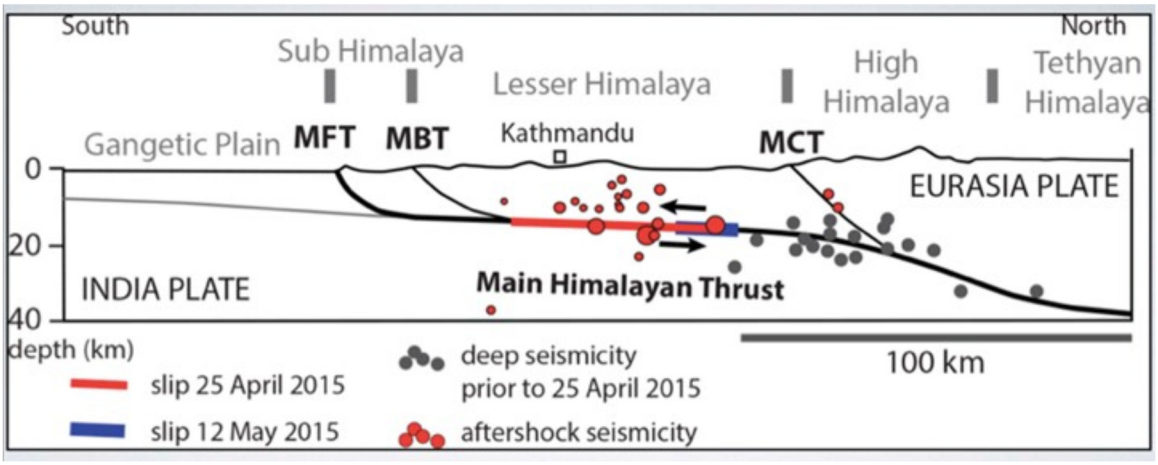

Figure 2.1 Generalized cross section through the Central Himalaya showing the flat-ramp-flat geometry of the MHT and the modeled slip of the Gorkha earthquake and May 12, 2015 aftershock (USGS 2015).

2.2 Earthquake setting

Nepal has a long history of destructive earthquakes. At least ten major earthquakes (Chitrakar and Pandey 1986) were recorded in the historical archives since the 13th century. The M7.8 Gorkha earthquake occurred on April 25, 2015 at 06:11:26 UTC on or near the main Himalayan thrust fault at 28.1473 N latitude and 84.7079 E longitude with a hypocentral depth of 15 km. There were five aftershocks with magnitude larger than 6.0, one of which was a M7.3 event that occurred on May 12, 2015 approximately 140 km east of the mainshock epicenter. Despite the large magnitude of the M7.8 Gorkha earthquake, and the very short epicentral distance of downtown Kathmandu, the ground motions recorded in the middle of the basin had a very low peak ground acceleration, PGA = 0.16g

and a very long period (5s) predominant pulse. Unfortunately, the earthquake sequence was poorly recorded, and only one strong motion instrument (KATNP) managed by the USGS has so far provided ground motion time-series over the bandwidth of engineering interest.

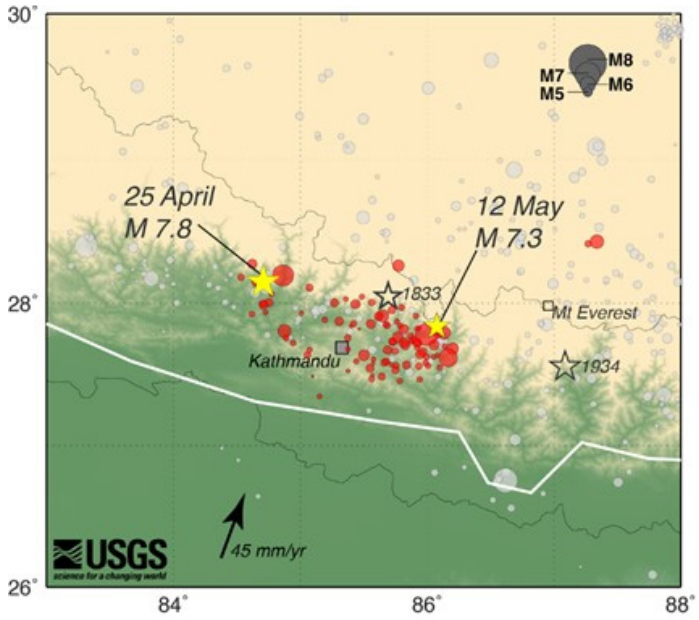

Figure 2.2 Aftershock seismicity map for the April 25 event prepared by Robertson and Koontz (USGS).

2.3 Ground response

Given the magnitude of the M7.8 Gorkha earthquake on April 25, 2015, and the epicentral distance of the fault rupture from Kathmandu, that is, approximately zero, the mainshock ground motion was very atypical: it was characterized by a very long period (5s) predominant pulse that reverberated in the valley for 4-5 cycles before gradually decaying, and a very low high-frequency content, which together led to a surprisingly low peak ground acceleration (PGA) of 0.16g. Although the nature of the mainshock strong motions is still poorly understood, it explains to a large extent the surprisingly low extent of infrastructure damage within the basin, compared to the empirical predictions for a M7.8 earthquake below Kathmandu.

Severe damage has been observed adjacent to basin edges around the Kathmandu Valley after the April 25 M7.8 earthquake and subsequent aftershocks. The two main locations where the damage due to ground shaking is concentrated is in the center of the Kathmandu Valley, and the damage in the center of the valley is most likely due to site amplification caused by the sedimentary basin. Significant damage has also been observed along the basin edges, especially around Bhaktapur and Sakhu where most of the old structures were collapsed. At these locations the observed damage and higher intensity of the ground shaking (Figure 2.3b) is most probably an indicator of the influence of the basin edge effects.

(a) Siddhito (27°44'7.32"N 85°18'33.81"E); Kimdol (27°42'35.55"N 85°16'49.09"E); Sakhu (27 43' 49.5"N 85 27' 52"E); Bakhtapur (27 40' 13.2"N 85 25' 48.8"E).

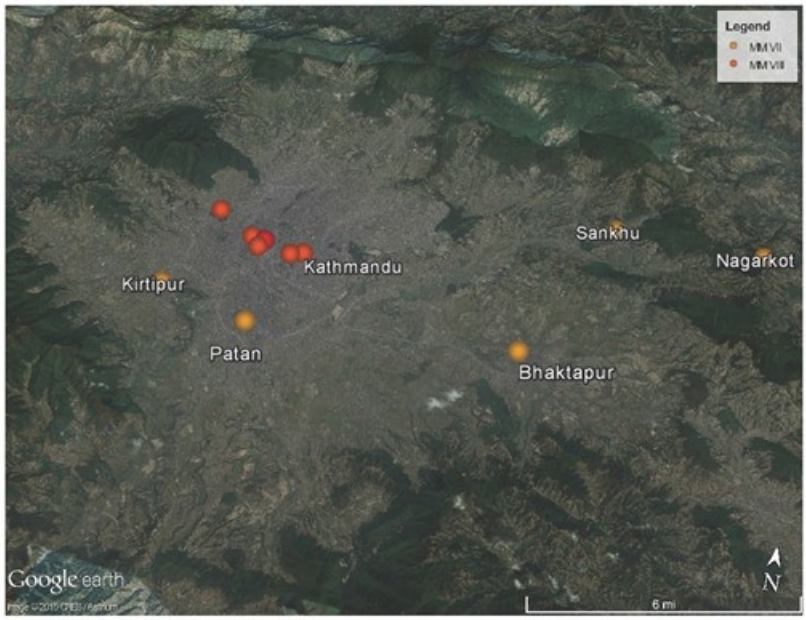

(b) Orange MMI=VII, Red MMI=VIII.

Figure 2.3 Damage distribution in the Kathmandu Valley: (a) primary locations of observed building damage (after Hashash et al. 2015); (b) Modified Mercalli Intensities assigned to main cities in the Kathmandu Valley (GeoNames.org).

Topography effects dominated to a large extent the ground response and ground failures effects observed during the M7.8 Gorkha earthquake sequence, that is the structural damage and ground failure (slope stability failure) distribution patterns. Structural damage was specifically concentrated at the top of isolated hills within the valley, at hilltops within and surrounding the edges of the Kathmandu Valley (Figure 2.4), and at the hilltops and ridge crests of the mountainous countryside.

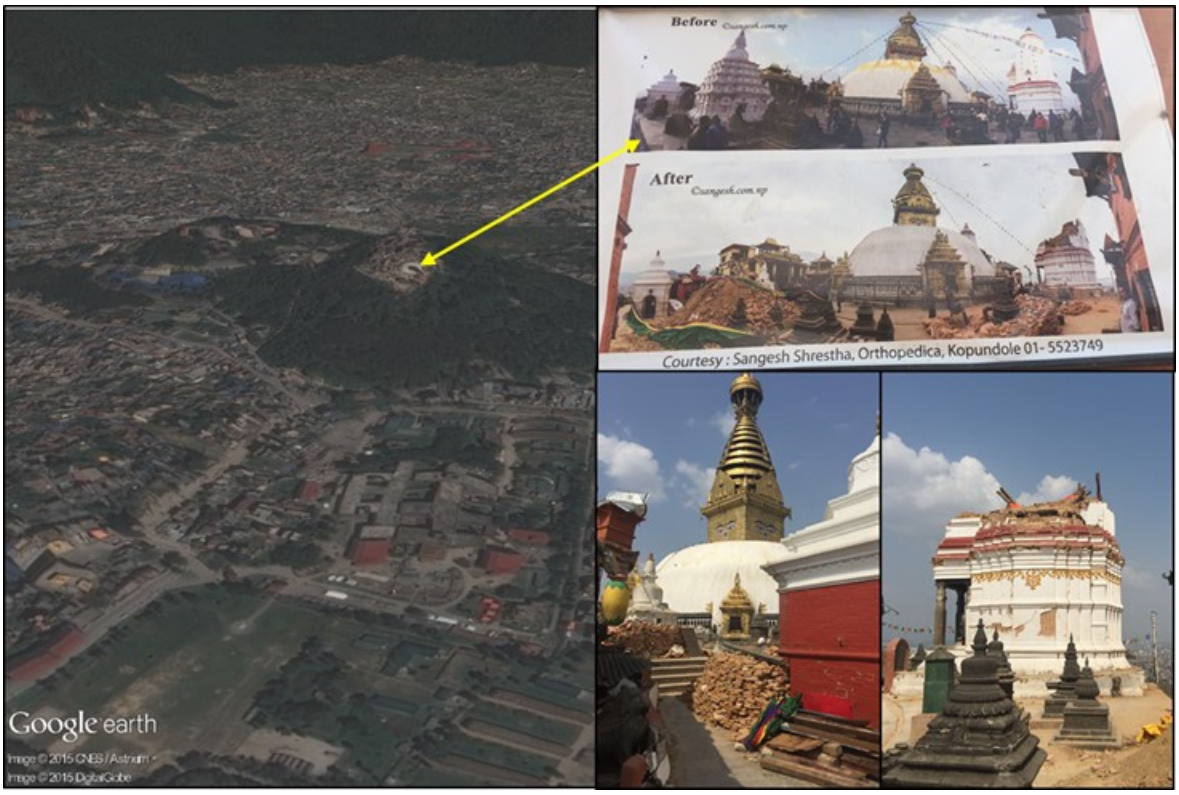

Figure 2.4 Damage in Swayambhu (Monkey) Temple (27.715270 N, 85.290231 E) (after Hashash et al. 2015).

2.4 Slope stability and landslides

With elevations in Nepal ranging from 100m to 8,848 m above mean sea level from south to north over a distance of approximately 120 km, topographic relief is exceptional and the characteristically steep slopes are vulnerable to landslides. The April 25, 2015 earthquake and its related aftershocks triggered significant landsliding that killed hundreds of people, blocked several roads, buried villages, and dammed natural rivers. Interpretation of satellite imagery taken prior and subsequent to the earthquake by the GEER team indicates that the earthquake triggered more than 6,000 new or reactivated landslides within the Sindhupalchok District alone (Ziselsberger 2016). An example of pre-and-post earthquake satellite imagery is shown in Figure 2.5.

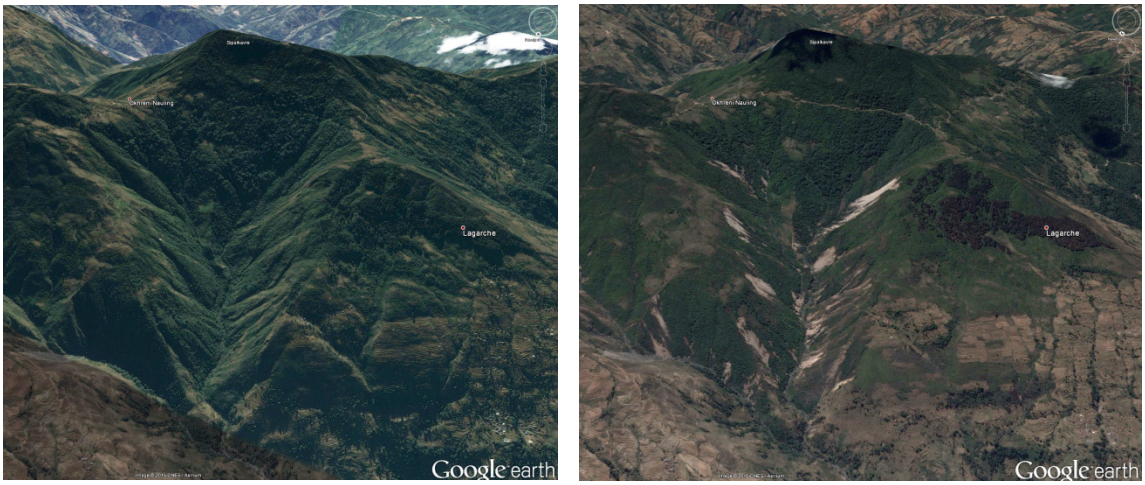

(a) (b)

Figure 2.5 Satellite imagery from: (a) December 2014; (b) May 2015 (27°52'3.57"N, 85°39'5.41"E). Light scars in right image indicate areas of earthquake-induced landsliding (after Hashash et al. 2015).

A more comprehensive description of the landslides from this event can be found in Collins and Jibson (2015). A landslide fissure was observed at the ridge of Ramkot Village, which is located at the edge of the Kathmandu Valley (Figure 2.6). The extensive fissure is more than 15 cm wide.

Figure 2.6 Head scarp observed on the ridge of the slope triggered by the 2015 earthquake (after Hashash et al. 2015).

Figure 2.7 Charikot-Lamabagar road sector affected by landslides triggered due to the earthquake .

Figure 2.8 Gabion retaining walls that did not perform well along the Charikot-Lamabagar Road.

Figure 2.9 Landslides observed along the road alignment constructed along steep terrain.

Figure 2.10 Large scale landslides that affected the Charikot-Lamabagar Road sector.

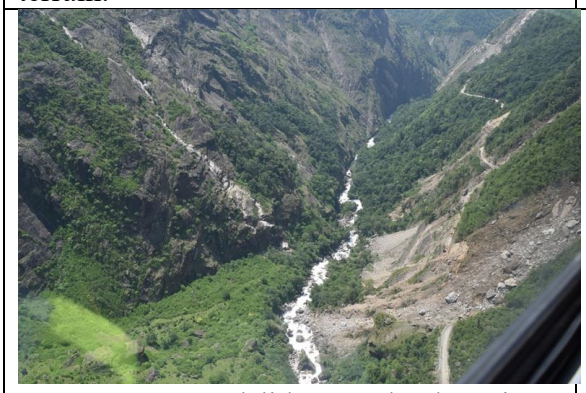

Figure 2.11 Landslide near the dam site of the hydropower project that damaged the road.

Figure 2.12 Landslides observed along dam site of the Upper Tamakoshi Hydropower project.

(Figures 2.7-2.12 after Hashash et al. 2015)

Figure 2.13 Rockfall upstream of the hydropower project (after Hashash et al. 2015).

A landslide dam was observed at Pandise, located in the Sertung Village Development Committee of the Dhading District (Figure 2.14). The landslide occurred at Ankhu Khola, a tributary of the Budi Gandaki River. The slope gradient of the tributary was approximately 30-35^{o}, and large boulders traveled down the tributary of Ankhu Khola, blocking the river channel for about a week (Figure 2.15). The landslide dam was breached naturally.

Figure 2.14 A landslide dam at the tributary of Ankhu Khola right after the 2015 Gorkha earthquake main shock (28°40.6'0"N, 83°59.8'0"E).

Figure 2.15 Debris mass from the left bank of the river that caused the landslide damming.

(Figures 2.14 and 2.15 after Hashash et al. 2015)

Figure 2.16 The landslide blocked the Kali Gandaki River forming approximately 2 km long and 150 m deep artificial lake (28°24'8.48"N, 83°35'47.5"E) (after Hashash et al. 2015).

2.5 Liquefaction and cyclic soil failure

The Kathmandu Valley contains lake and river sediments that, when shaken, can deform due to either cyclic failure or liquefaction. Ground failures due to weak soils were almost exclusively in the Kathmandu Valley. The weak soils that caused ground damage ranged from fine sands to silty sands to silty clays. In some locations, the ejecta indicated clear evidence of liquefaction as the controlling failure mechanism. As an example, sand boils were observed in an empty plot of land (Figure 2.17). This site is located about 90m northeast of a meandering river; it is elevated above the floodplain.

Figure 2.17 Liquefaction ejecta in agricultural field. Material was very fine, primarily silt with some sand. No damage to the building in the background (27.711025°N, 085.262290°E) (after Hashash et al. 2015).

According to the locals, the ground flooded during the earthquake and remained flooded for two days. Locals also claimed that other plots in the vicinity liquefied, but surface effects of liquefaction were not evident elsewhere. Auguring on this site revealed that the soil profile generally consists of interbedded layers of loose fine sand and silt up to 2.5m depth. The water table was located approximately 3m below the ground surface.

The Tsho Lorpa glacial lake dam is a natural lake located at an elevation of 4,535m (Figure 2.18). A spillway was built to control the water level in the lake and prevent overtopping and possible breaching of the natural dam. The site was visited by helicopter to examine the integrity of the natural dam material around the lake (Figure 2.19) as well as the spillway (Figure 2.20). The natural dam material showed no cracking or slumping. At the spillway, lateral spreading was observed on the lake side. Significant lateral and vertical displacement (Figure 2.21) are observed in excess of a total of approximately 1.5m laterally and 0.5 m vertically.

Figure 2.18 Plan view of Tsho Lorpa Glacial Lake Dam (27°52'9.57"N, 86°27'44"E) (after Hashash et al. 2015).

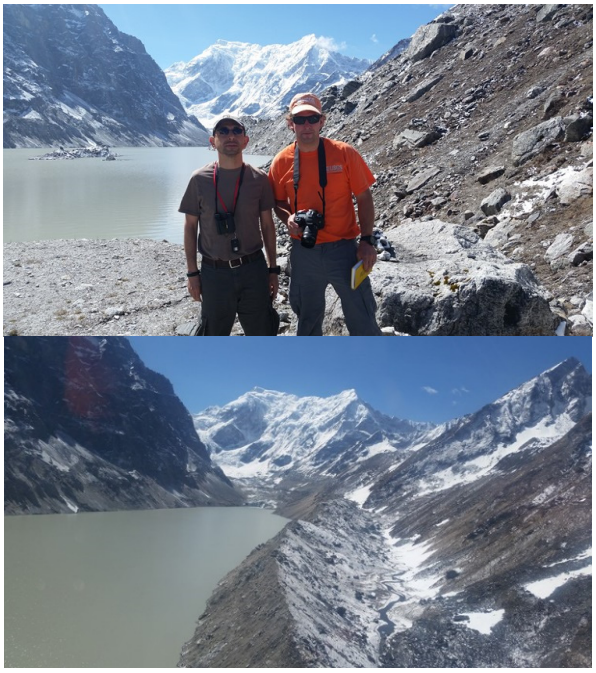

Figure 2.19 Glacial Lake (27°52’9.57”N, 86°27’44”E) (after Hashash et al. 2015).

Figure 2.20 Spillway of Glacial Lake (27°52’9.57”N, 86°27’44”E) (after Hashash et al. 2015).

Figure 2.21 Lateral Spreading along the upstream side of the spillway (27°52'9.57"N, 86°27'44"E) (after Hashash et al. 2015).

2.6 Performance of dams and hydropower facilities

The April 25 mainshock and May 12 aftershock damaged six projects of the Nepal Hydroelectric Authority, totaling approximately 190 Megawatts (MW) of generating capacity, and 10 projects by independent power producers, totaling over 80 MW of capacity (Hyrdroworld 2015). One dam was visited, at the Upper Tamakoshi Power Plant, which had unique damage features.

The 456 MW Upper Tamakoshi Power Plant was considered the national priority project, since upon completion, it will be the largest hydroelectric project in Nepal. The earthquake-induced ground shaking caused excessive settlement in the headworks resulting in an interruption in the construction schedule. According to the Upper Tamakoshi Power Plant authorities, 4cm of settlement occurred after a M5 earthquake on December 18, 2014. Settlement increased to 12 cm and 18 cm after the April 25 mainshock and the May 12 aftershock, respectively (

b). On April 27 a landslide induced by the April 25, 2015 earthquake closed the access road to the headworks. The earthquake also toppled a gabion wall used as a cofferdam/diversion structure (Figure 2.22c). Rockfalls were observed in the headworks area (Figure 2.22d). The very steep left and right abutments may create further landslide hazard at the site (Figure 2.22e).

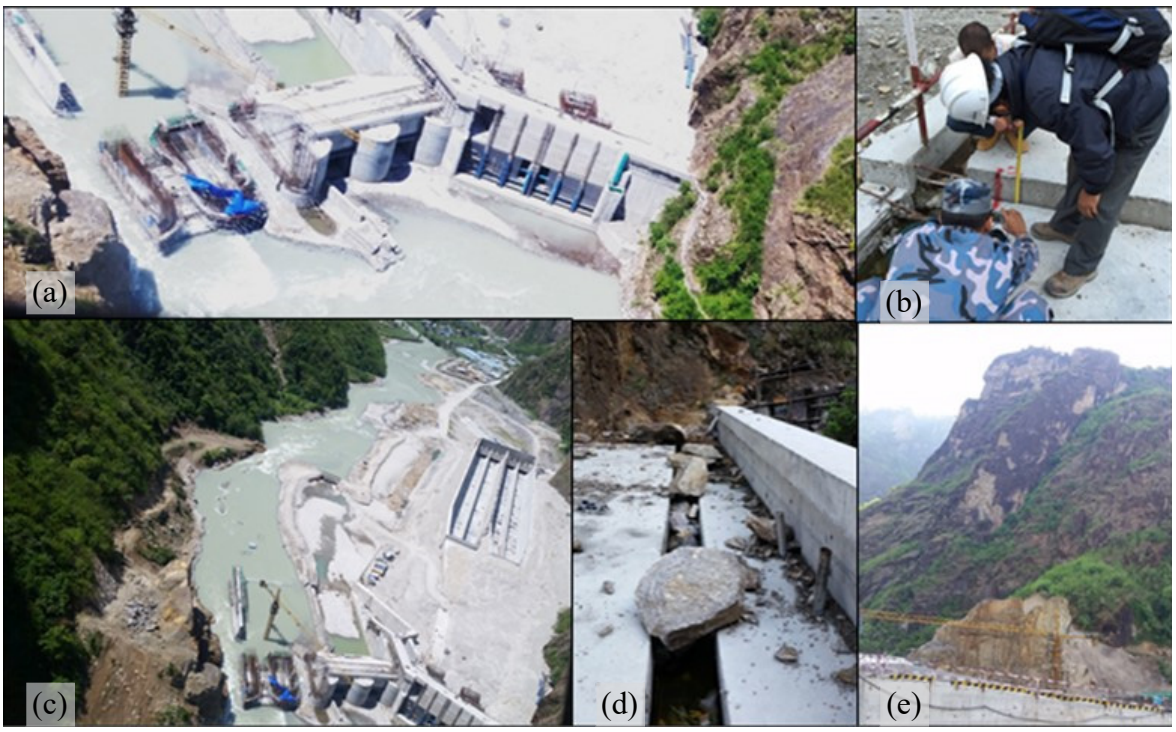

Figure 2.22 Damage observed at the Upper Tamakoshi Power Plant: (a) Aerial image of the headworks; (b) settlement at the headworks; (c) breached cofferdam; (d) rockfalls; (e) steep slopes at the abutments (27°55’29.8’’N, 86°12’46.4’’E) (after Hashash et al. 2015).

STRUCTURAL RESPONSE OF BUILDINGS

Three broad building classifications are used in Nepal: wood-framed construction, unreinforced load-bearing masonry (URM) wall construction and reinforced-concrete (RC) frame construction. All building types experienced damage and collapse as a result of the earthquake sequence. The investigation documented in this report focused on RC frame buildings, which exhibited a wide range of performance from minor damage to complete collapse. Additional observations related to RC frame buildings, as well as to wood-framed and URM buildings can be found in documentation from the Earthquake Engineering Research Institute (EERI) reconnaissance team (Lizundia et al. 2015).

A Government of Nepal report estimated that 6,613 RC frame houses collapsed and 16,971 RC frame houses were damaged in the earthquake sequence (Nepal 2015). The statistic are striking, but they pale in comparison to the numbers of collapsed and damaged masonry houses, 492,239 and 239,726, respectively (Nepal 2015). Although masonry construction was more heavily affected, examination of RC frame construction is still imperative since it is a critical building sector. The observations presented here are divided into two broad groups: low-rise to mid-rise buildings and high-rise buildings. The low-rise to mid-rise building observations are subdivided into two additional groups: common residential / commercial buildings, which have no engineering and minimal planning, and institutional buildings (such as government or university buildings), which typically were more carefully planned and may have incorporated basic engineering considerations.

3.1 Low-rise to mid-rise reinforced concrete frame buildings

Typical low-rise to mid-rise RC frame buildings suffered from a wide range of deficiencies that negatively impacted seismic performance. Chief amongst these is the lack of an enforced building code. Even simple rules of thumb established over two decades ago (Nepal 1994a and 1994b) appear to be almost universally ignored. The range of deficiencies includes: poor material quality, no inspection or quality control, very light column reinforcement (longitudinal and transverse), no ductile detailing in beam-column joints and potential hinge regions, pervasive and severe geometric irregularities, buildings constructed beyond permitted height and heavy brick masonry infill. Masonry infill is not intended to be structural, but it is built tight against the RC frame, and as a result, significantly affects structural earthquake response. In addition to the structural damage described below, extensive damage to infill masonry was also observed.

3.1.1 Common residential / commercial buildings

In Kathmandu, RC frame construction is used extensively for buildings with residential, commercial and combined residential / commercial function. These buildings are typically constructed by the owners in an ad hoc fashion with irregular structural layouts, using minimal steel reinforcement and whatever materials are available on site to mix concrete. Extensive non-ductile seismic response was observed for this class of building, with the

Balaju region of Kathmandu hit particularly hard. Representative observations from Balaju are presented in this section.

Figure 3.1 RC frame building with upper-story collapse; Balaju, Kathmandu: (a) overall view showing vertical irregularity; (b) zoomed-in view showing collapsed story.

Figure 3.1 shows a building with collapsed stories in the upper portion of the structure. (Note that for these and all subsequent photographs, GPS coordinates are provided in Appendix A.) The response of this building was likely affected by the adjacent shorter building, which was built tight up against its taller neighbor. This shorter building significantly stiffened the lower three stories and focused soft / weak story collapse at the vertical irregularity. Figure 3.2 shows a building that experienced soft / weak story collapse at the base of the building, which tipped and was subsequently arrested by a neighboring building. Figure 3.3 shows a building being demolished by hand after experiencing a multi-story pancake collapse. Residents of the neighborhood reported that this building survived the main shock and all occupants evacuated safely, but subsequently collapsed during a small aftershock. Figure 3.4 shows a building with a larger plan area that developed pancake collapses in the first and second stories. The columns contained light transverse reinforcement at large spacing, which led to shear failure and longitudinal bar buckling.

Figure 3.2 RC frame building with first-story collapse; Balaju, Kathmandu: (a) overall view showing first story collapse; (b) zoomed-in view showing contact with adjacent building.

Figure 4.3 RC frame building with multi-story pancake collapse; Balaju, Kathmandu.

Figure 3.4 RC frame building with pancake collapse in first and second stories; Balaju, Kathmandu: (a) overall view of building; (b) zoomed-in view of column failure.

Figure 3.5 RC frame building with severe damage, but no collapse; Balaju, Kathmandu: (a) overall building view showing soft / weak first story due to drive-in bay; (b) zoomed-in view of partial first story; (c) zoomed-in view of column with shear failure.

Some RC frame buildings sustained severe damage, but did not collapse. For example, Figure 3.5 shows a multi-story residential building that has extensive degradation in the first story. (In these photos, North is to the left.) The first story was effectively softer / weaker than the upper stories due to the drive-in bay in half of the story, which did not contain masonry infill. In the other half of the first story, the partial masonry infill influenced the response. At the corner column, a hinge developed at the column base, with more damage evident on the outside of the building, which was the compression side when the building was being pushed to the North (Figure 3.5b). For loading in the North direction, this corner column was separated from the lower region of masonry infill (below the windows), such that the column effective height extended from ground to the top of the window region. This corner column did not develop a shear failure. In contrast, the center column was constrained by the masonry infill above and below the window region, and the reduced effective height caused the column to fail in shear (Figure 3.5c). However, the building did not collapse, and the damaged column reveals more tightly spaced transverse reinforcement (less than one column depth) than was observed in most other damaged / collapsed buildings. In Figure 3.5c, also note the development of a flexural hinge at the top of an interior column, which was not constrained by masonry infill. The damage pattern and post-earthquake lean of this building indicate that demand may have been more heavily concentrated in the North direction at this site.

Demonstrating the marked variability in response within close proximity, Figure 3.6 shows a more ornate multi-story residential building that sustained only non-structural masonry damage and beam-column joint shear failure, but did not collapse. The damaged beam-column joint reveals only one visible transverse bar and longitudinal bar buckling.

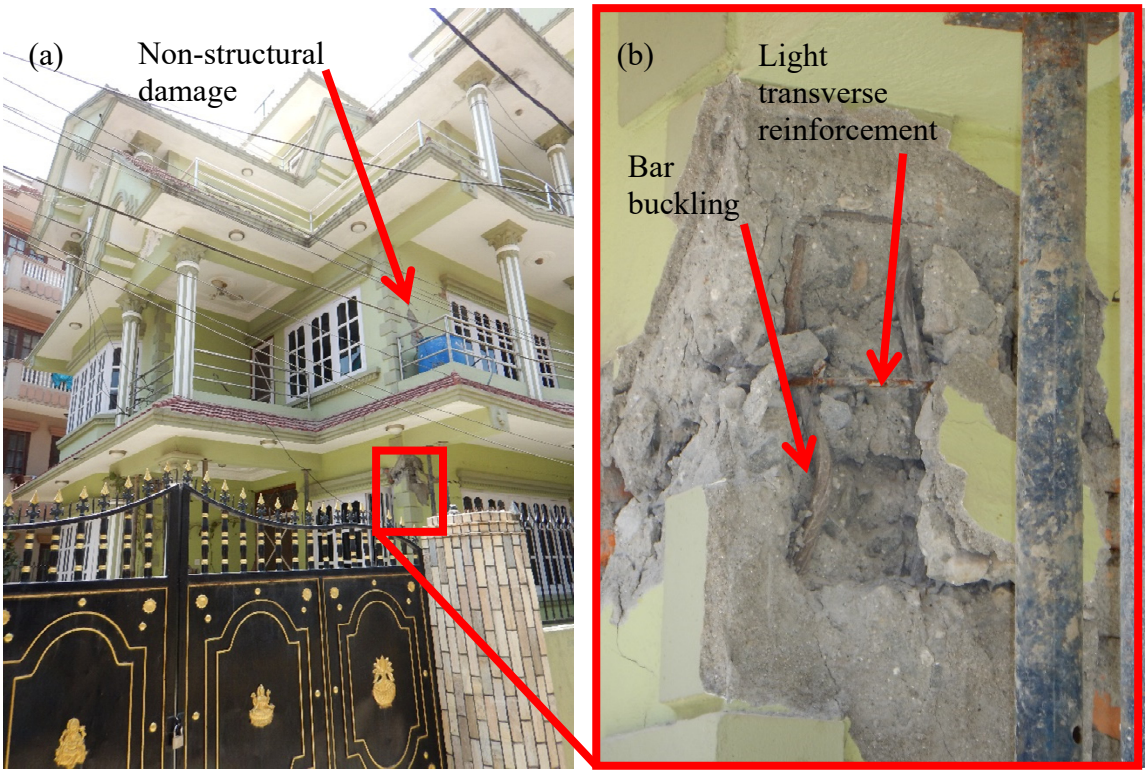

Figure 3.6 RC frame building with significant damage, but no collapse; Balaju, Kathmandu: (a) overall view; (b) beam-column joint failure.

3.1.2 Developed residential / commercial buildings

Although the majority of low-rise to mid-rise RC frame buildings in Kathmandu are owner-constructed with minimal formal planning, several mid-rise buildings visited were relatively new structures that had been more carefully developed, likely with some engineering input.

Figure 3.7 Valachhen Building, RC frame with structural and non-structural damage: (a) exterior elevation view; (b) column shear falure; (c) nonstructural masonry damage; (d) column shear failure.

One such structure is the Valachhen Building shown in Figure 3.7a, which was roughly two years old at the time of the earthquake. This building is located in the Harisiddhi region of Kathmandu, and it is situated on a ridge and built on a steep slope. Although the construction details and quality in the Valachhen Building appeared to be better than in the common RC frame buildings where severe damage and collapse were widely observed, significant structural and non-structural damage did occur. Shear cracking was evident in the non-structural masonry (Figure 3.7c), which was constructed tight up against the RC frame, and shear failure was observed in a structural column (Figure 3.7b and 3.7d). The shoring seen in these photos was placed after the earthquake. In addition, settlement was observed on the down-slope (back) side of the building. This building may have experienced larger ground shaking due to ridge amplification effects.

Constructed at roughly the same time as the Valachhen Building (2013), the Civil Trade Centre (CTC) Mall is a large shopping and entertainment complex in the Sundhara region of Kathmandu. The CTC Mall has two subgrade parking levels, nine primary stories and a rooftop penthouse level. As shown in the exterior views in Figure 3.8, it sustained damage to non-structural masonry, and localized structural damage was also observed.

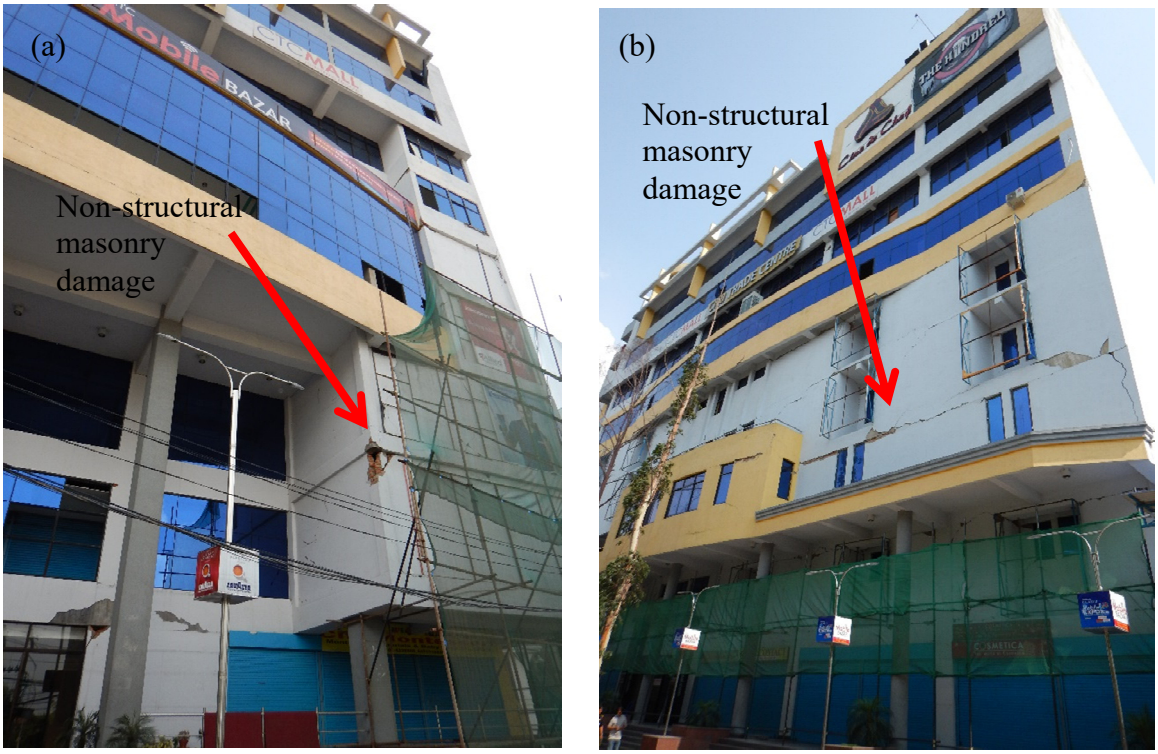

Figure 3.8 CTC Mall – exterior views: (a) view from east side (Kanti Path); (b) view from north side (China Town Road).

Structural damage in the CTC mall included concrete spalling at several column bases (Figure 3.9) and beam flexural cracking (Figure 3.10). On the west side of the building (away from Kanti Path), several inches of building settlement was observed. On the east side of the building, adjacent to Kanti Path, the backfill at the main entrance settled several inches. Near the center of the building, in plan, an interesting damage event was observed. The concrete elevator enclosure was terminated above the slab of the bottom

basement level, and the bottom portion of the elevator enclosure was brick masonry (Figure 3.11a). Although the elevator enclosure was not intended to participate structurally for lateral load resistance, it did attract demand during the earthquake, and the overturning effects from the elevator enclosure were not effectively resisted by the relatively weak masonry portion at the bottom of the enclosure. As a result, these overturning demands were transmitted to the concrete girders of the first basement level, and shear cracks developed near the girder support (Figure 3.11b) while flexural cracks developed in the girder span (Figure 3.11a), although collapse did not occur. The shoring seen in these photos was placed after the earthquake.

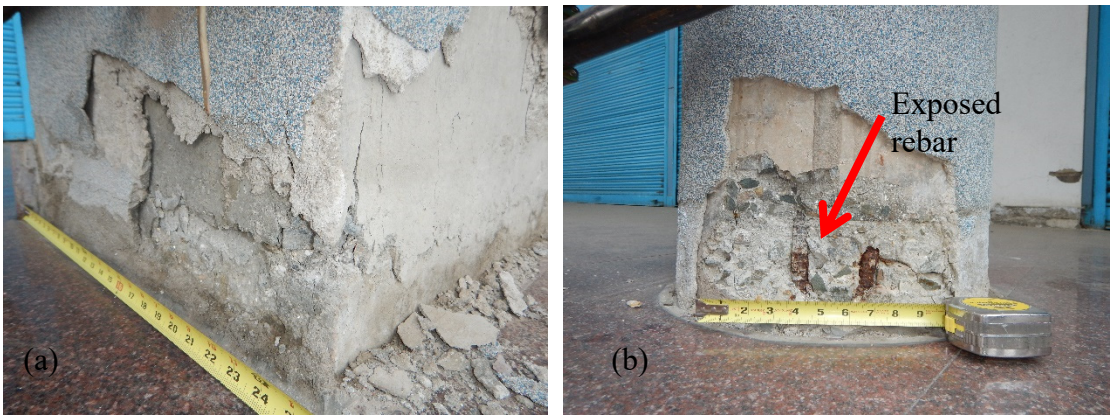

Figure 3.9 CTC Mall – concrete spalling at column bases: east side of building; (b) north side of building.

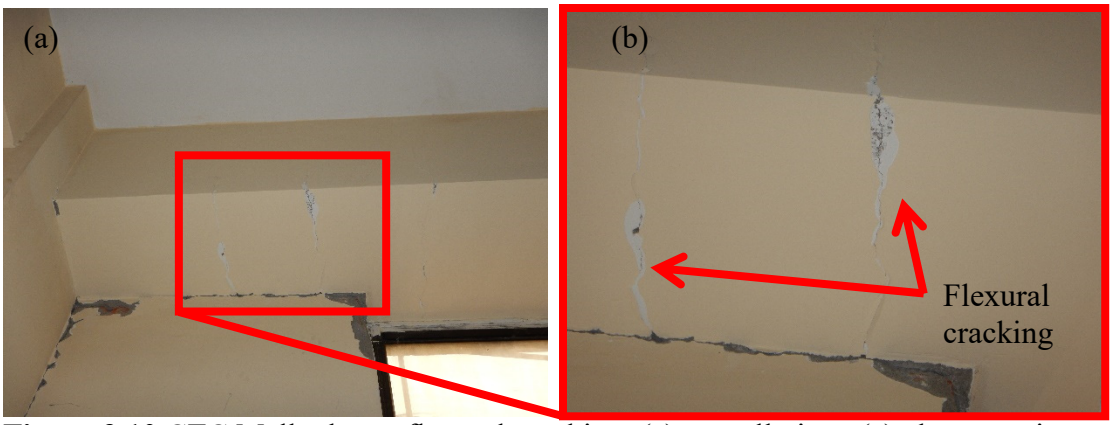

Figure 3.10 CTC Mall – beam flexural cracking: (a) overall view; (c) close-up view.

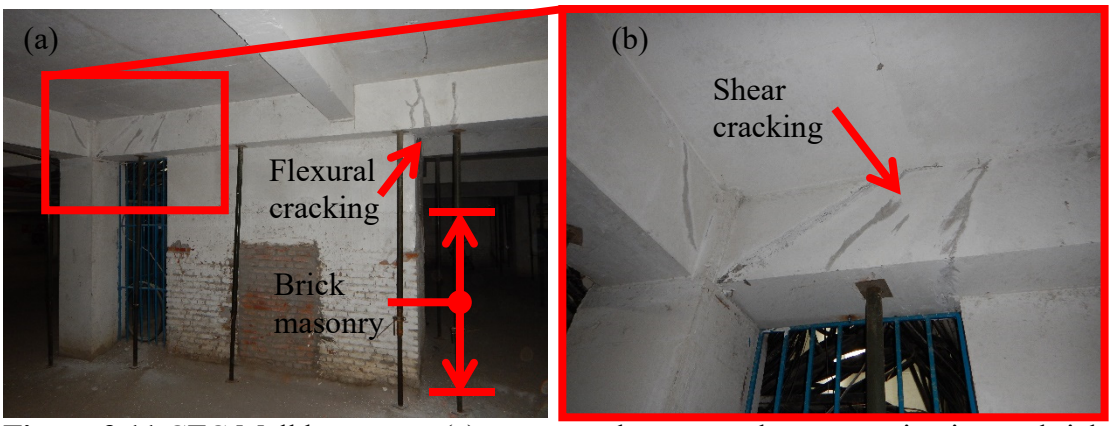

Figure 3.11 CTC Mall basement: (a) concrete elevator enclosure terminating on brick masonry; (b) close-up of beam shear cracking.

In contrast to the significant damage observed in the Valachhen Building and the CTC Mall, two new buildings, which were designed by Pumori Engineers, were observed to have only very minor non-structural damage. The buildings are directly adjacent to each other, and one (6-story) was finished and occupied at the time of the earthquake (Figure 3.12a), whereas the other (8-story) was under construction (Figure 3.12b).

Figure 3.12 New buildings designed by Pumori Engineers: (a) occupied 6-story building; (b) 8-story building under construction.

Slight cracking occurred on a very limited basis in non-structural masonry walls. No structural damage was observed, and the well-conceived structural design was illustrated by a particular detail in the basement of the buildings. As shown in Figure 3.13,

for the finished 6-story building, clerestory windows at the top of the basement level allow light into the basement. This is a common scenario, and as will be shown below for a different building, it can lead to "short column" shear failure at the clerestory windows. In these buildings, the structural engineer intentionally did not allow the windows to extend to the column edges, but instead designed column extensions adjacent to the windows to provide additional shear resistance and prevent column shear failure (Figure 3.13).

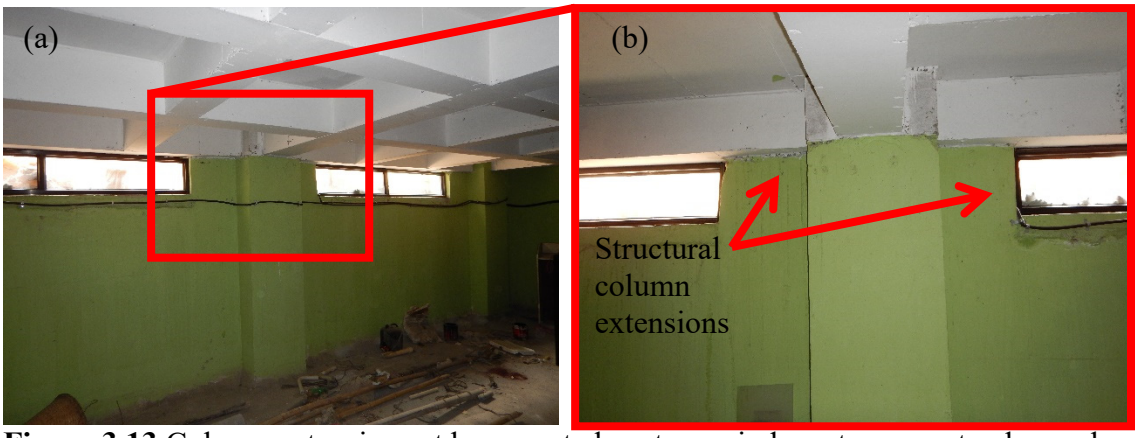

Figure 3.13 Column extensions at basement clerestory windows to prevent column shear failure in short column region: (a) overall view; (b) close-up view.

3.1.3 Institutional buildings

In addition to being used extensively in residential / commercial buildings in Kathmandu, RC frame construction is also used in institutional buildings, such as government and university facilities. Several examples are provided below. Since these buildings have more specific programmatic requirements as compared to the common residential / commercial sector, they typically have more regularity and have been more carefully planned. Although they still had deficiencies and exhibited non-ductile response, as will be shown below, the construction quality and detailing appear to be more similar to the developed residential / commercial buildings described above and better than the commonplace residential / commercial buildings described above.

The Government of Nepal Central Fisheries Building, which houses the Directorate of Fisheries Development under the Ministry of Agricultural Development, is located in the Balaju region of Kathmandu, in close proximity to the heavily damaged and collapsed common residential / commercial buildings described above. As shown in Figure 3.14, this two-story building has a RC frame structure that is visually much stouter than the common residential / commercial buildings discussed above. Although the building survived the earthquake sequence, it did still sustain significant structural damage, which was concentrated in the first story. The second story had minimal structural damage. As shown in Figure 3.15, major damage was observed at the base of one corner column, and less visible shear cracking was observed at other column base locations. Figure 3.16 shows close-up views of representative shear failures that were observed at the tops of the first story columns in multiple locations throughout the building. Non-structural infill framing may have influenced the column response and reduced the effective height of the columns and contributed to the shear failures (Figure 3.16c).

Figure 3.14 Central Fisheries Building – exterior view.

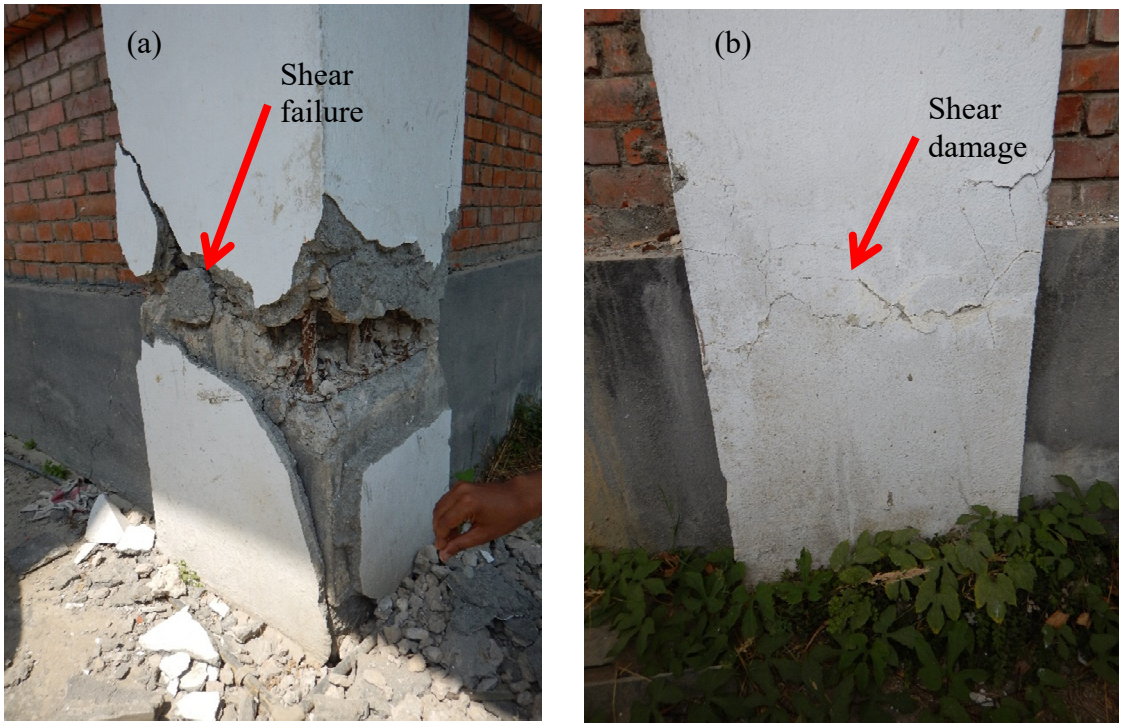

Figure 3.15 Central Fisheries Building – column base damage: (a) corner column; (b) exterior column.

Figure 3.16 Central Fisheries Building – column shear damage at top of first story: (a) interior; (b) exterior; (c) exterior overall; (d) exterior close-up.

Short-column effects were also noted on the Thapathali campus of Tribhuvan University in the Block E Building, which was opened in 1998. Like the new buildings described above, the Block E Building had clerestory windows at the top of the basement.

However, these columns were not reinforced like the columns in the new buildings (Figure 3.13) and they exhibited shear damage (Figure 3.17). In Figures 3.17a and b, concrete cover was chipped off to conduct post-earthquake inspection. Although the shear damage was evident, it was not nearly as pronounced as in other buildings, such as the Central Fisheries Building. Following the earthquake sequence, Tribhuvan University had evacuated the Block E Building, but officials were considering retrofit strategies to enable reoccupation.

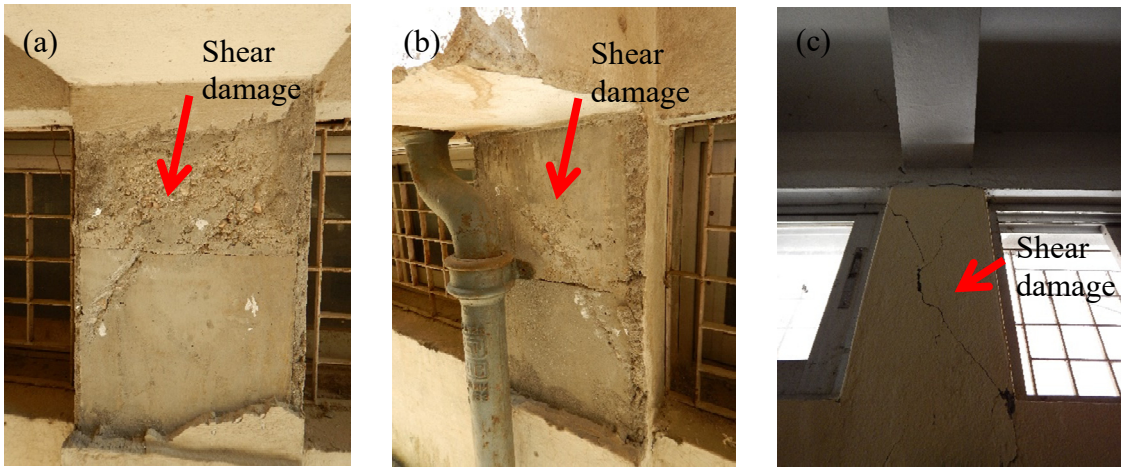

Figure 3.17 Tribhuvan University Thapathali Campus Block E Building – short column shear damage: (a) exterior; (b) exterior; (c) interior.

Figure 3.18 Kathmandu Engineering College Block C Building – exterior view.

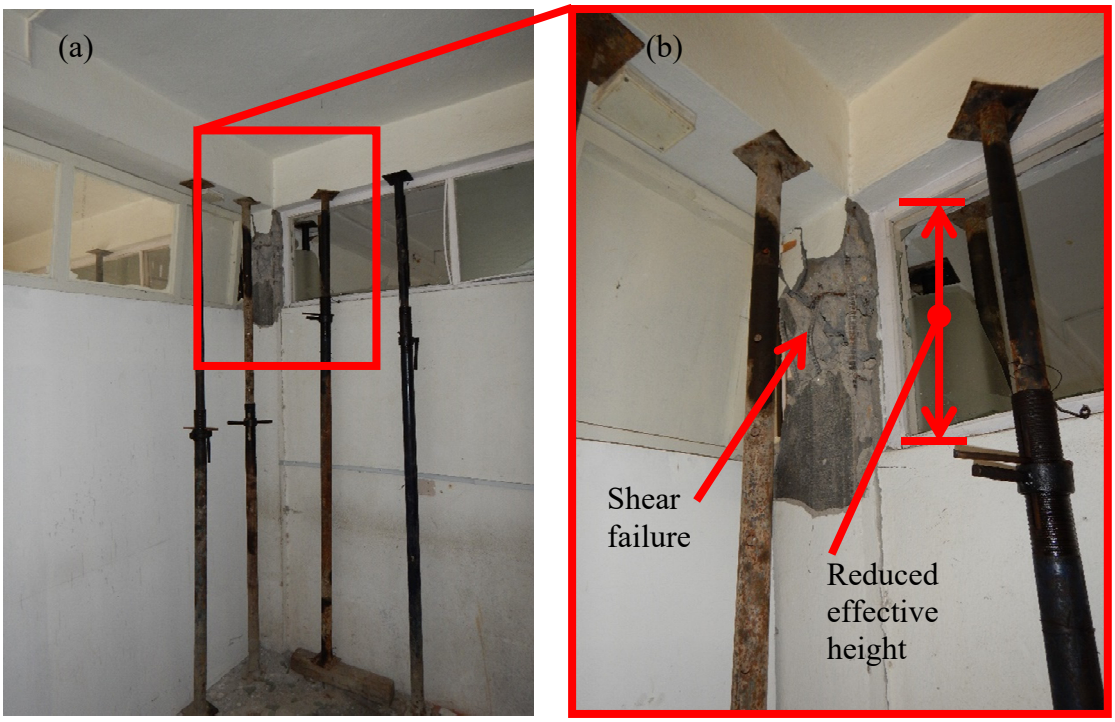

Figure 3.19 Kathmandu Engineering College Block C Building – short column shear failure: (a) overall view; (b) detail view.

Figure 3.20 Kathmandu Engineering College Block C Building – short column shear failure.

On the campus of Kathmandu Engineering College (KEC), short column effects were responsible for column shear failure in the 4-story Block C Building, which was constructed in 1983. As shown in the exterior view in Figure 3.18, windows extended over the majority of the stories at the building perimeter, and the exterior columns were not damaged. However, on the interior, partial-height non-structural masonry walls were below windows that allowed natural light to penetrate into interior spaces, and column shear failure occurred in the short span within the window region (Figures 3.19 and 3.20). Almost no transverse reinforcement was evident and longitudinal bar buckling occurred. The interior walls were predominantly placed in the east-west direction (long direction of the building), so column response in the north-south direction primarily occurred over the full clear story height without constraint from the interior walls. The KEC Block C Building formed a first-story mechanism, with the remaining stories exhibiting no observable structural damage. The shoring seen in these photos was placed after the earthquake.

In contrast to the KEC Block C Building, the KEC Block E Building (Figure 3.21), which is a six-story structure constructed in 2003, sustained only very light non-structural damage to infill masonry. The Block E Building had a very similar configuration as the Block C Building, with full-height exterior windows and partial height non-structural interior masonry walls topped with windows to allow light penetration (Figure 3.22). In this case, the interior walls were predominantly placed in the north-south direction, which is the long direction of the building. Thus, the interior columns had significantly shortened spans in the north-south direction, but they suffered no ill effects.

Figure 3.21 Kathmandu Engineering College Block E Building – exterior view.

The difference in performance between the two KEC buildings is striking, particularly considering their proximity to each other and their similar configurations. The KEC campus map in Figure 3.23 shows the relative positions of Block C and Block E and

the nominally perpendicular orientations of their long directions. Several factors may have contributed to the difference in seismic performance. Block E is approximately 20 years newer than Block C, so it likely that the design and construction practices were better for Block E, such as the column extensions at the interior clerestory windows, similar to but not as pronounced as those in the new designs by Pumori Engineers (Figure 3.13). In addition, the short column effect was primarily in the east-west direction for Block C and the north-south direction for Block E. Thus, ground shaking directionality may have played a role, with east-west shaking possibly being more severe at this particular site.

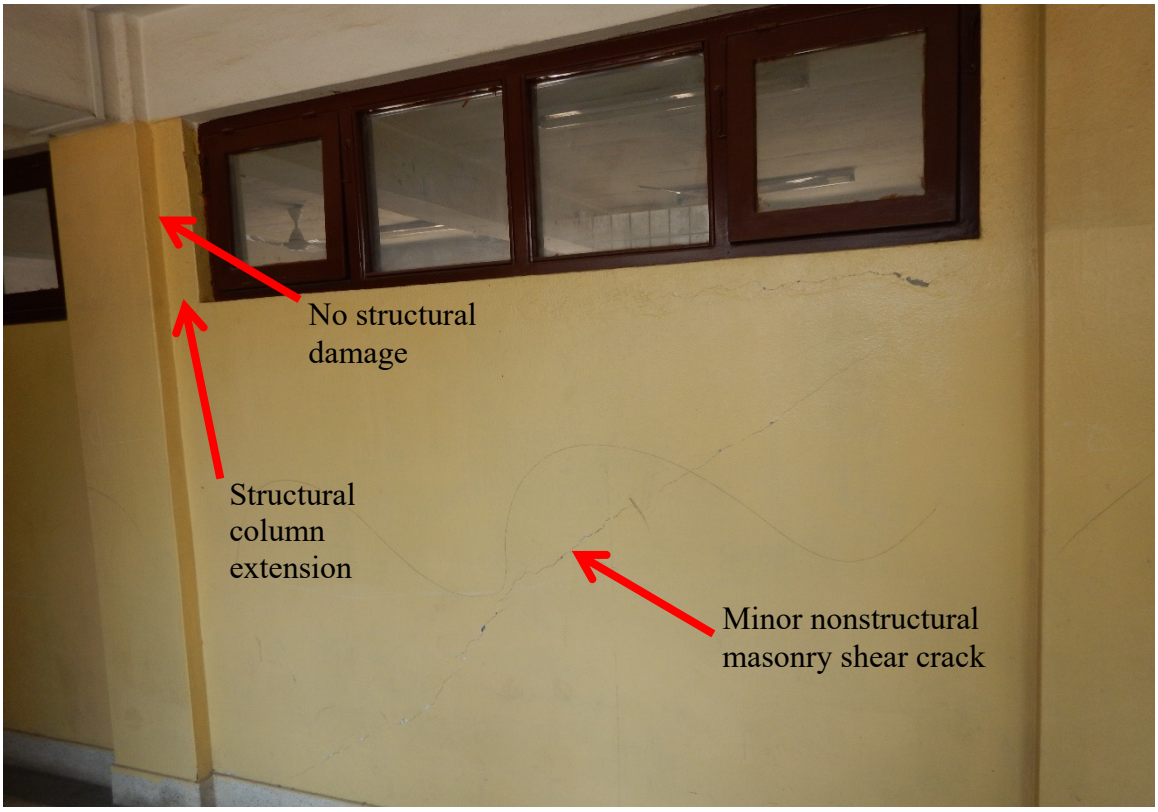

Figure 3.22 Kathmandu Engineering College Block E Building – interior view.

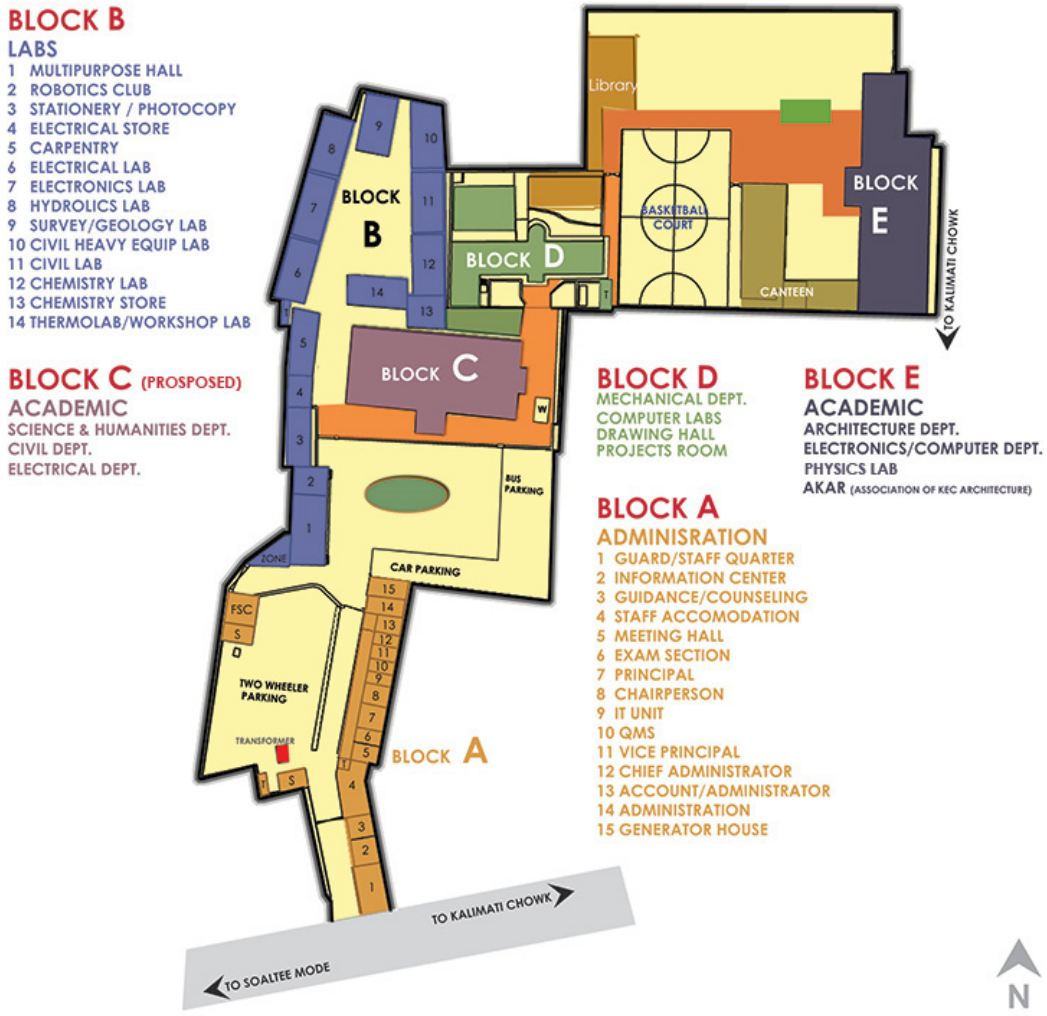

Figure 3.23 Kathmandu Engineering College Campus Map (KEC, 2016).

3.2 Mid-rise to high-rise reinforced concrete frame buildings

Although low-rise construction has been dominant in Kathmandu for many years, mid-rise to high-rise construction (roughly 10 to 20 stories) has been used more recently for apartment buildings. These tall apartment buildings, largely opened within the past five years, are primarily RC frame structures, but they may also employ RC shear walls for lateral load resistance. Generally speaking, these mid-rise to high-rise buildings exhibited adequate structural performance during the earthquake sequence (no collapse and relatively modest structural damage), but they also experienced significant non-structural damage, including pounding. Although the primary structural systems of these buildings are proportioned, detailed and constructed according to more rigorous earthquake-resistant standards, brick masonry is still used extensively for non-structural walls and architectural features, and this masonry was heavily damaged during the earthquake sequence, presenting a safety risk and necessitating major post-earthquake repair work. Observations

from post-earthquake inspection of several mid-rise to high-rise RC apartment buildings are presented below. Table 3.1 summarizes primary information about the apartment complexes and the observed damage.

Table 3.1 Summary of mid-rise to high-rise buildings inspected.

Building Complex	Maximum # of Stories	Notes
Cityscape	13	Moderate non-structural damage
Mero City	18	Moderate non-structural damage, structural damage not known, under construction
Parkview Horizon	20	Heavy non-structural damage, structural damage not known
Silver City	18	Moderate to heavy non-structural damage, light structural damage, pounding
Sun City	17	Moderate non-structural damage (2 buildings), light non-structural damage (3 buildings)
Swayambhu	12	Moderate to heavy non-structural damage, backfill settlement around buildings

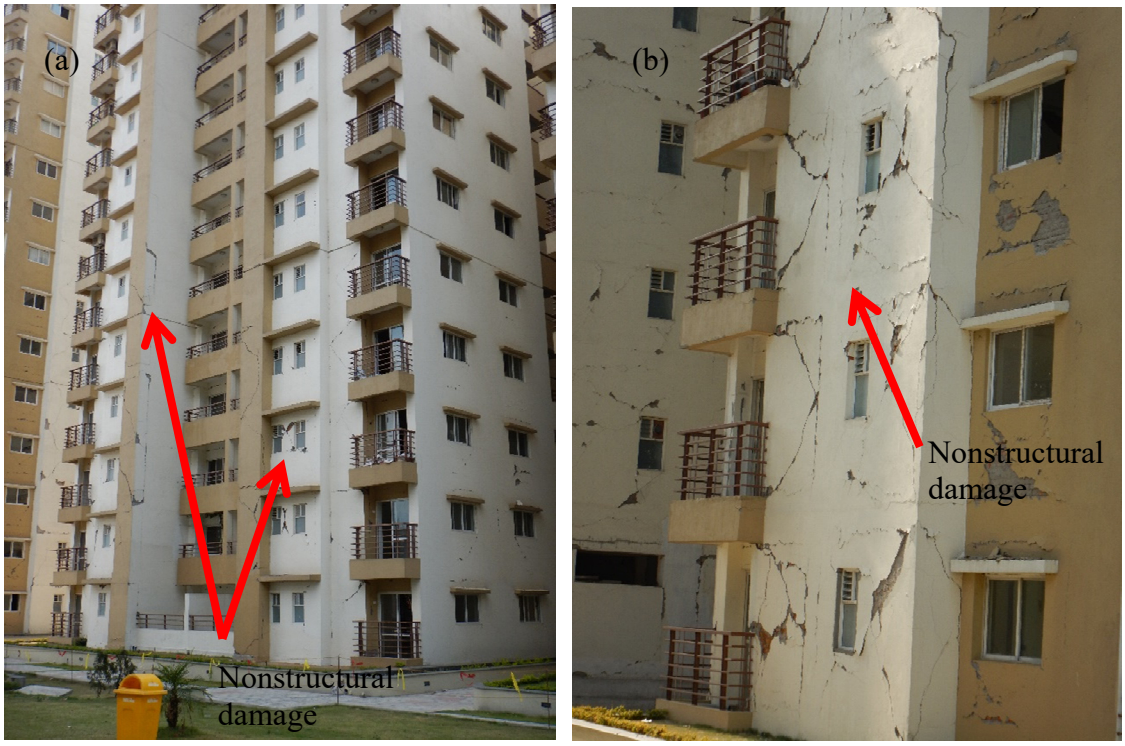

Figure 3.24 Cityscape – moderate non-structural damage: (a) overall view; (b) detail view.

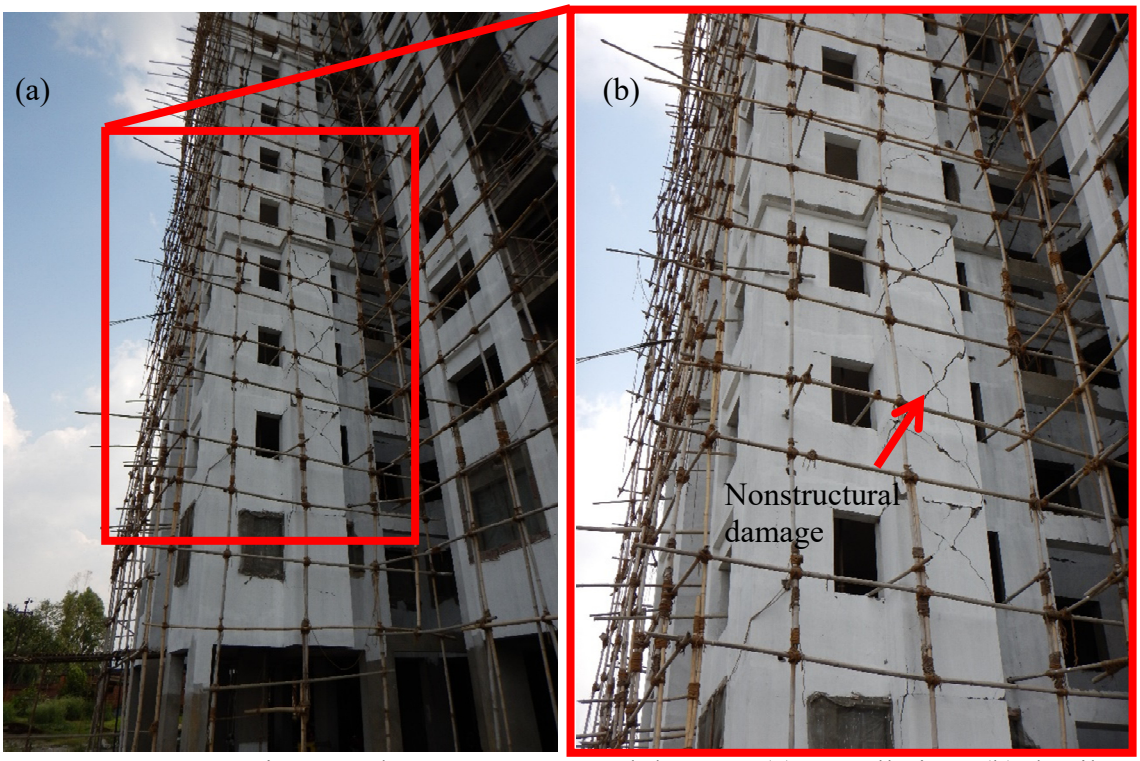

Figure 3.25 Mero City – moderate non-structural damage: (a) overall view; (b) detail view.

Cityscape is a large residential development with low-rise and high-rise buildings, including four towers. The towers sustained moderate non-structural damage (Figure 3.24) but no structural damage was observed. Similar shear damage of non-structural masonry infill was observed in the Mero City complex, which was under construction at the time of the earthquake (Figure 3.25). Much more severe non-structural damage was observed at the Parkview Horizon complex (Figure 3.26), which consists of five towers built on the side of a hill. Whereas Cityscape and Mero City only developed diagonal cracking in non-structural masonry walls, Parkview Horizon had entire walls collapse, windows fall out, extensive falling debris around the building, and many portions of the buildings were left hanging precariously in danger of further collapse after the earthquake. A little over a month after the main shock, repair and rehabilitation efforts were underway at Cityscape, but Parkview Horizon remained inaccessible due to the serious safety concerns.

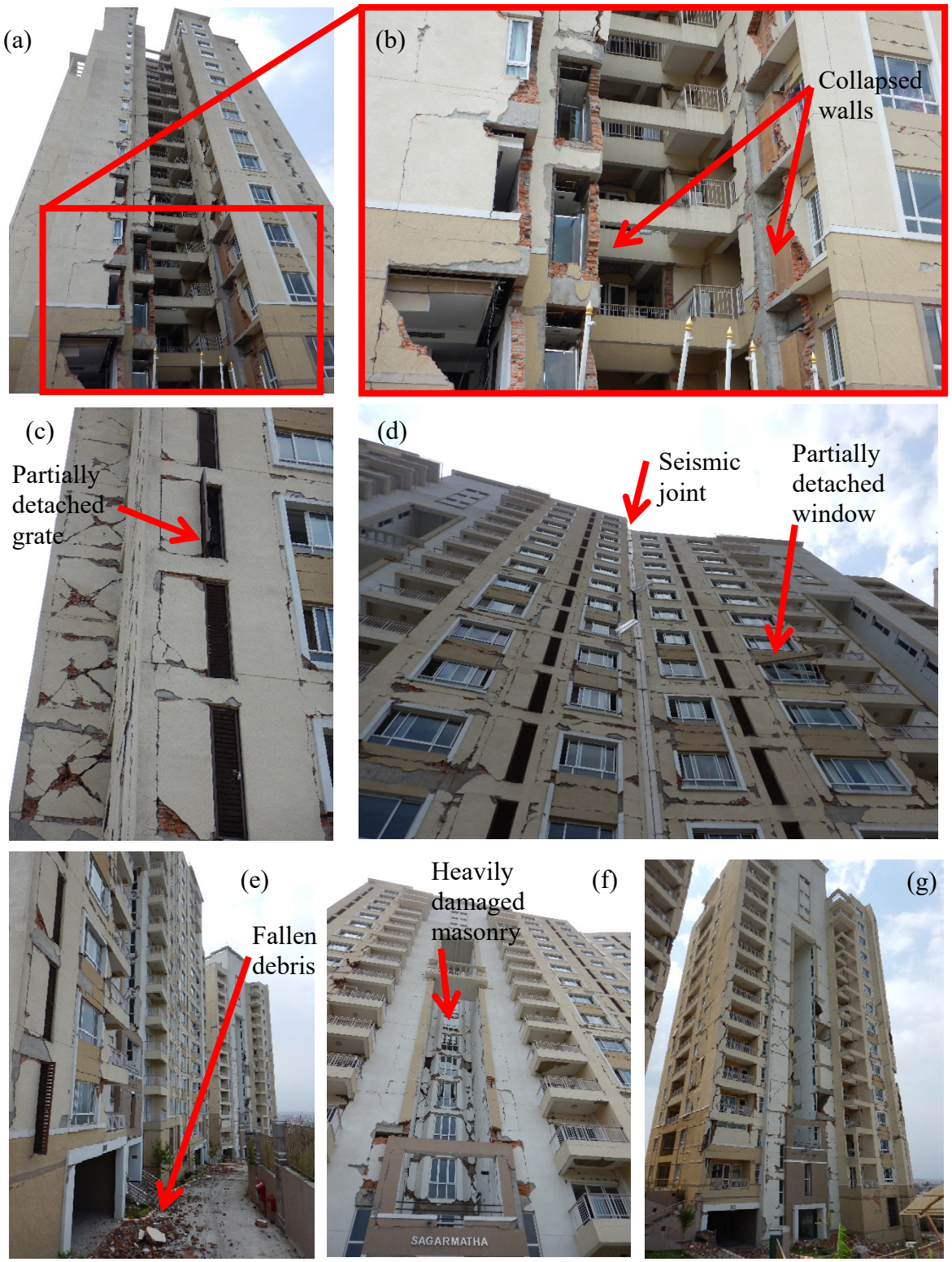

Figure 3.26 Parkview Horizon (Dhapasi) – heavy non-structural damage: (a) overall view Sagarmatha building east side; (b) close-up view Sagarmatha building east side; (c) northeast corner Sagarmatha building; (d) seismic joint between Sagarmatha and Kanchanjunga buildings; (e) looking along north side of complex; (f) north side of Sagarmatha building; (g) north side of Makalu building.

Figure 3.27 Silver City Apartment Complex.

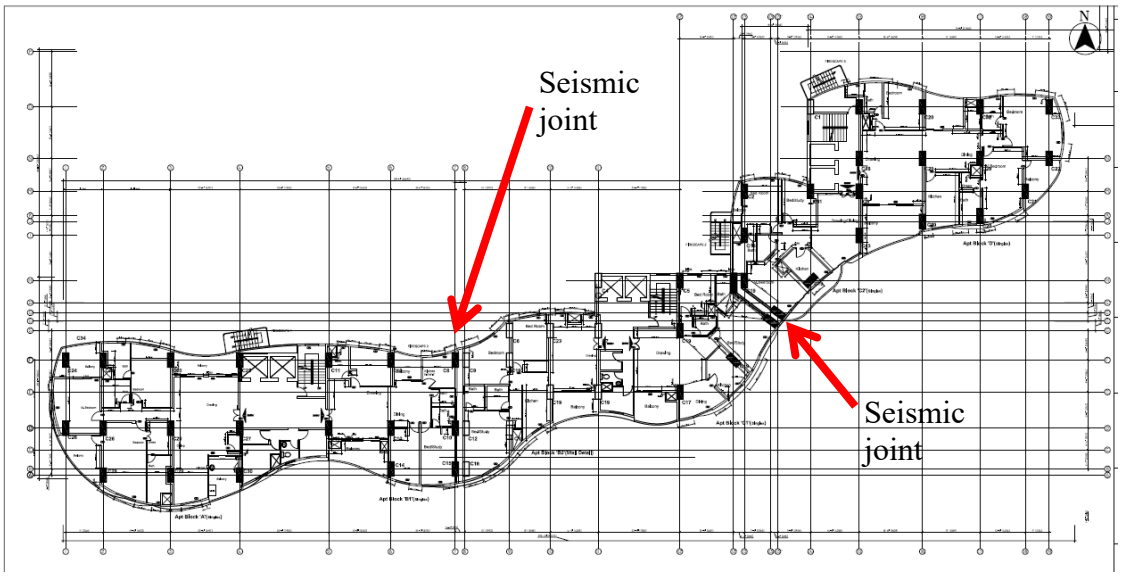

Figure 3.28 Silver City Apartment Complex – occupied building (drawing courtesy of Bimal Poddar).

Figure 3.29 Silver City Apartment Complex – seismic joints: (a) south view of west joint, straight; (b) south view of east joint, irregular; (c) top view of east joint, irregular; (d) interior view of east joint, irregular.

In the Kalikasthan region of Kathmandu, the Silver City Apartment complex is one of the tallest in the city and it sits at one of the highest points of the city. The complex comprises two buildings, one of which was still under construction at the time of the earthquake (Figure 3.27). The portion of the complex under construction is shown at the left of Figure 3.27 and was not inspected. The occupied building is actually composed of

three structurally independent units separated by seismic joints (Figure 3.28). As shown in figure 3.28, one of these joints is straight (north-south) and the other is irregular, with the primary portion of the joint oriented northwest-southeast and a short segment at the northwest end turning north-south. Photographs of the two joints are also shown in Figure 3.29.

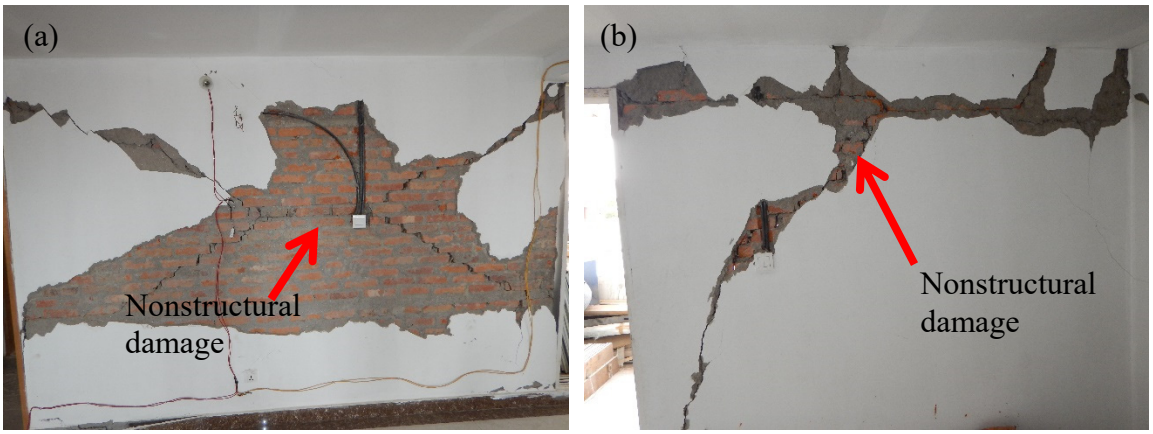

Figure 3.30 Silver City Apartment Complex – interior non-structural masonry wall damage in east-west direction.

Figure 3.31 Silver City Apartment Complex – exterior non-structural masonry wall damage: (a) base; (b) upper stories around windows and reentrant corners.

Silver City suffered moderate to heavy non-structural damage, although not as severe as Park Horizon. Figures 3.30 and 3.31 show representative damage to interior and exterior masonry walls, respectively. In general, the damaged regions were fairly contained

and did not present significant hazard due to falling or precarious partially-attached pieces. The primary exception to this observation is related to pounding between the independent structural units (Figure 3.32). Pounding caused significant damage to the roof parapets, and masonry and concrete debris was present at the base of the building in the seismic joints. Pounding occurred at both the straight and irregular joints, but it was particularly exacerbated at the irregular joint, which significantly reduced the effective clearance below the nominal dimension of 16 inches. Despite this damage, a little over a month after the main shock, repair and rehabilitation efforts were underway at Silver City.

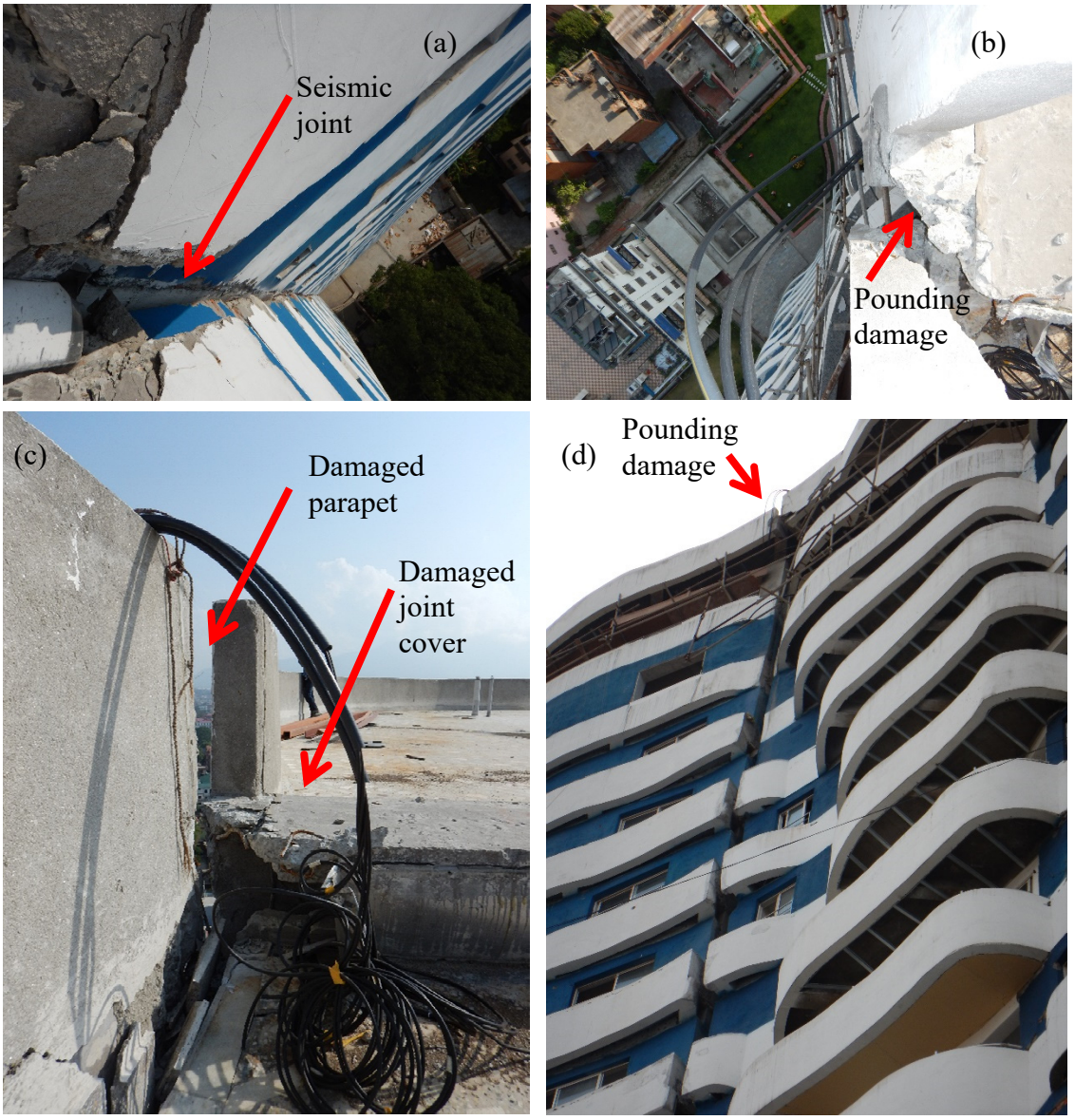

Figure 3.32 Silver City Apartment Complex – pounding damage: (a) looking down north side of east joint; (b) looking down south side of east joint; (c) detailed view top of east joint; (d) looking up at south side of east joint.

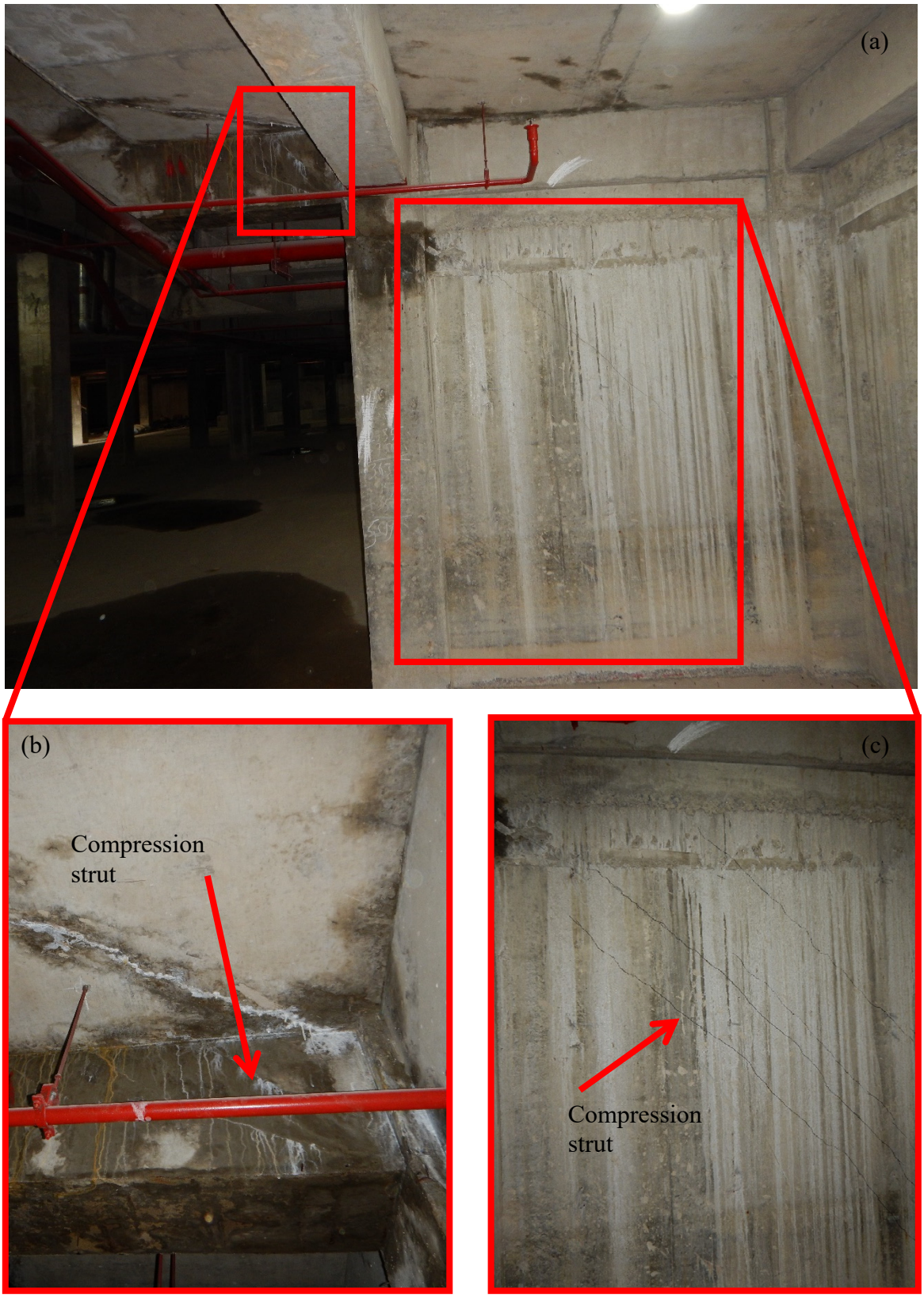

Figure 3.33 Silver City Apartment Complex – cracking in basement joint and wall: (a) overall view; (b) joint detail; (c) wall detail with cracks marked for clarity.

One interesting occurrence of minor structural damage was observed in the basement level below the south side plaza adjacent to the Silver City towers. This minor damage was cracking in several concrete joints and structural basement walls, which simply indicates the development of compression struts that were transferring lateral load from the plaza slab, which acted as a diaphragm to transmit inertial forces from the building down into the basement-level structure (Figure 3.33). This damage is not viewed as negative, but rather evidence of a reasonable subgrade lateral load path that developed, and was likely designed.

To the east of the Tribhuvan International Airport, the Sun City Apartment Complex is composed of five 17-story towers. These towers are situated in a group of three and a group of two (Figure 3.34), where seismic gaps of roughly 8 inches separated the adjacent independent structural units. The buildings are quite irregular in plan, with roughly five primary wings extending out from a central core area, and many reentrant corners. The Sun City towers provide an interesting comparison, since the group of three buildings, which was oriented on an axis running roughly northwest-southeast, suffered only very minor non-structural damage, while the group of two buildings, which was oriented on an axis running roughly east-west, suffered moderate non-structural damage (Figure 3.34). This damage was primarily characterized by diagonal shear cracking in masonry infill (Figure 3.35). The damaged portions remained stable and did not pose significant hazard during or after the earthquake. Repair efforts were in progress a little more than a month after the earthquake.

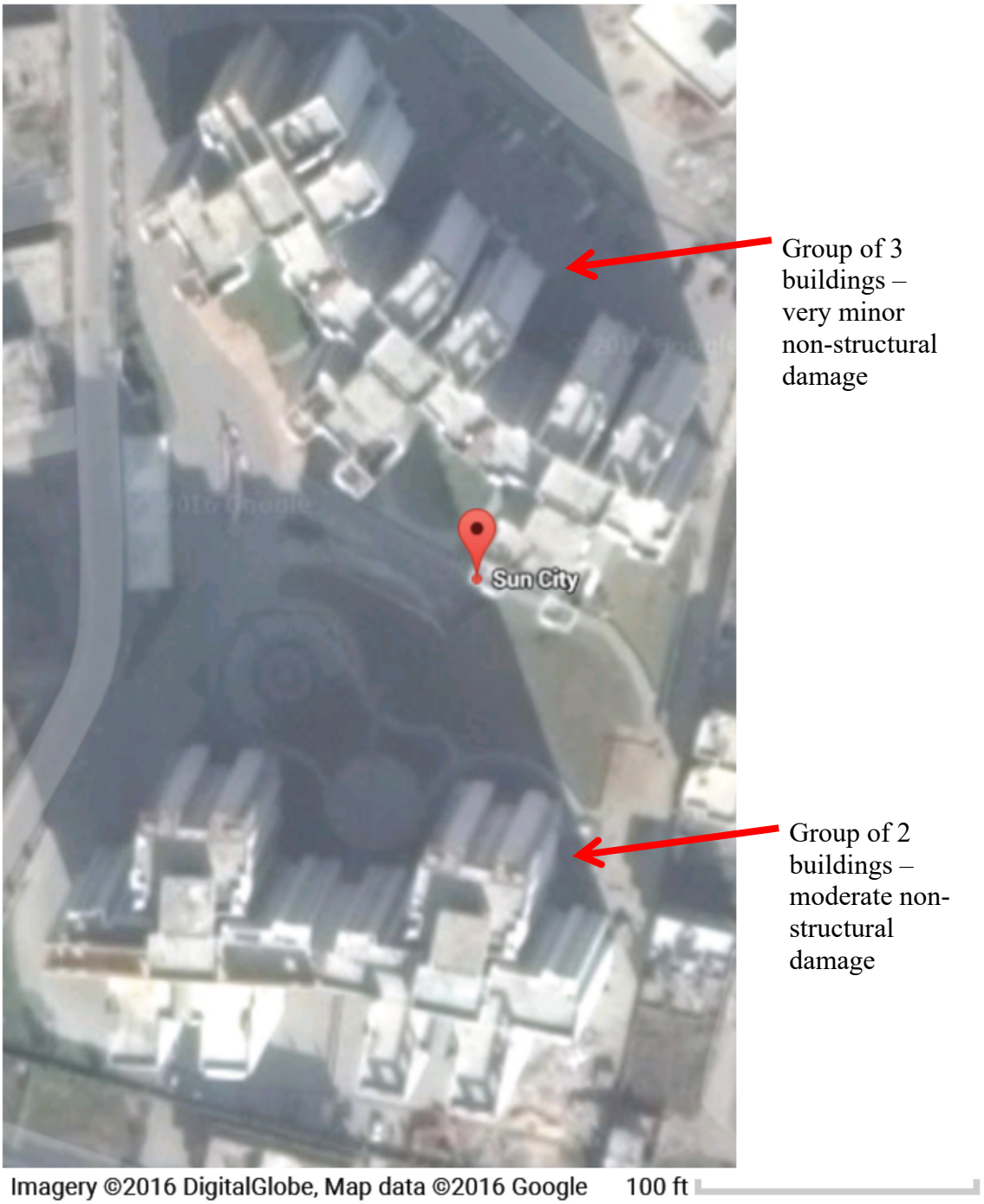

Figure 3.34 Sun City Apartment Complex (Google 2016).

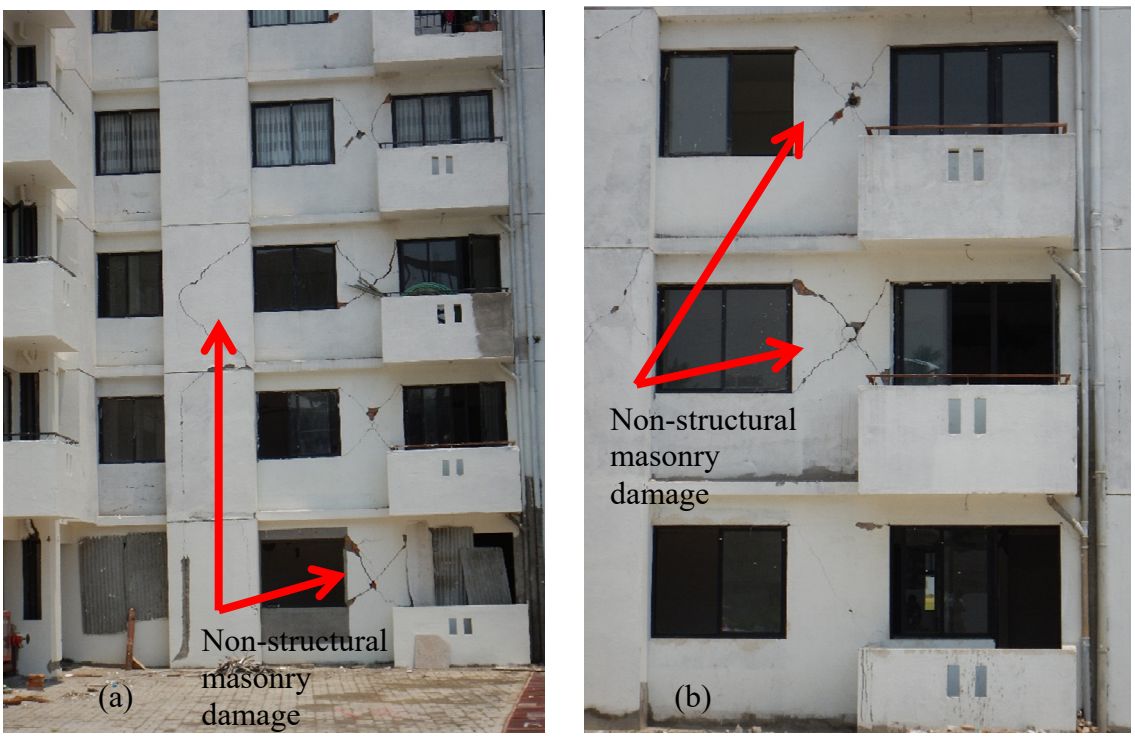

Figure 3.35 Sun City Apartment Complex – moderate non-structural damage in group of two buildings.

Figure 3.36 Sun City Apartment Complex – representative seismic joint: (a) overall view; (b) detail.

Also notable, particularly compared to Silver City, is the complete lack of pounding between adjacent towers. As shown in Figure 3.36, the seismic joint was roughly 8 inches at the narrowest, although it did widen towards the interior of the building. This joint is roughly half that provided at Silver City, where significant pounding was observed. This observation points to significantly different excitation at the Silver City and Sun City sites. Silver City may have been affected by local site effects or ridge amplification effects. In addition, the wide variation in response between the two groups of buildings in the Sun City complex indicates that the primary direction of shaking at the site was northeast-southwest, which is roughly one of the primary axes of the building triple set, but skewed roughly 45 degrees to the primary axes of the double set.

Figure 3.37 Swayambhu Apartment Complex.

The Swayambhu Apartment complex is a pair of towers located on a ridge, and locally built on a steep slope (Figure 3.37). The towers experienced moderate to heavy non-structural damage (Figure 3.38), which included extensive diagonal shear cracking and in some locations masonry walls became unstable and dislodged from the building. On the steep slope, settlement of backfill adjacent to the towers was also observed (Figure 3.39). Despite these indications of significant excitation at the site, no structural damage was observed in these buildings.

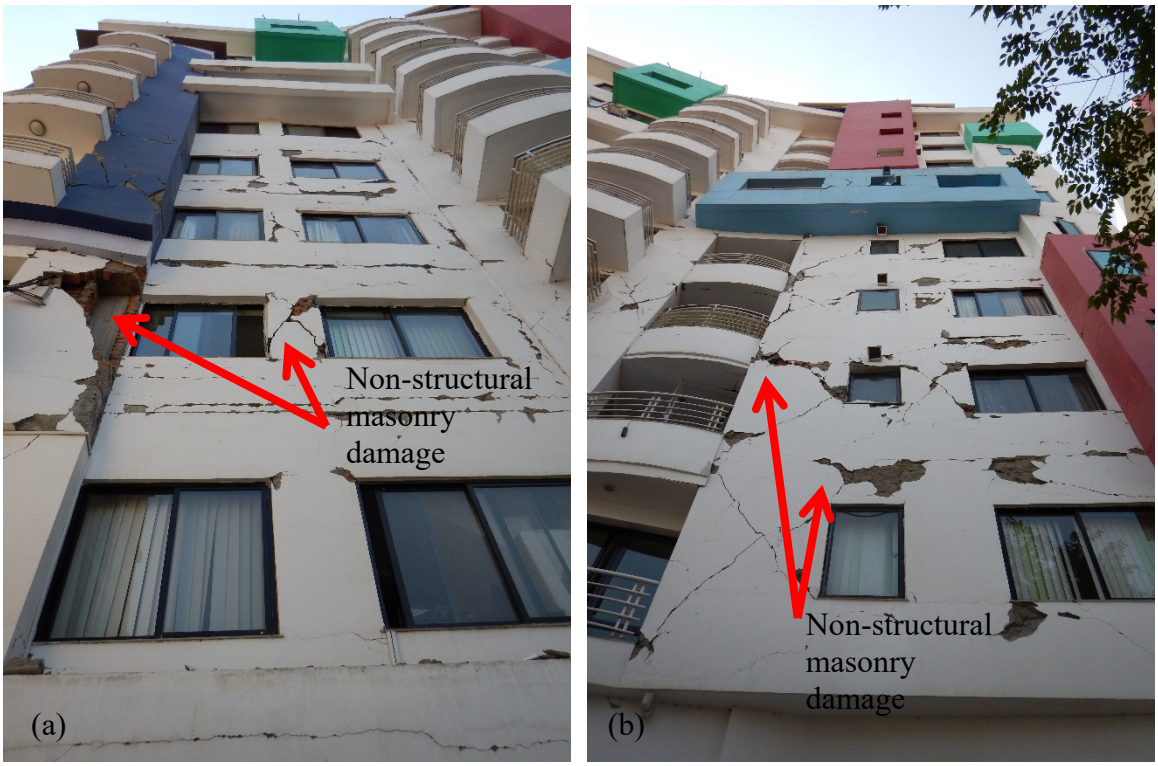

Figure 3.38 Swayambhu Apartment Complex – non-structural damage.

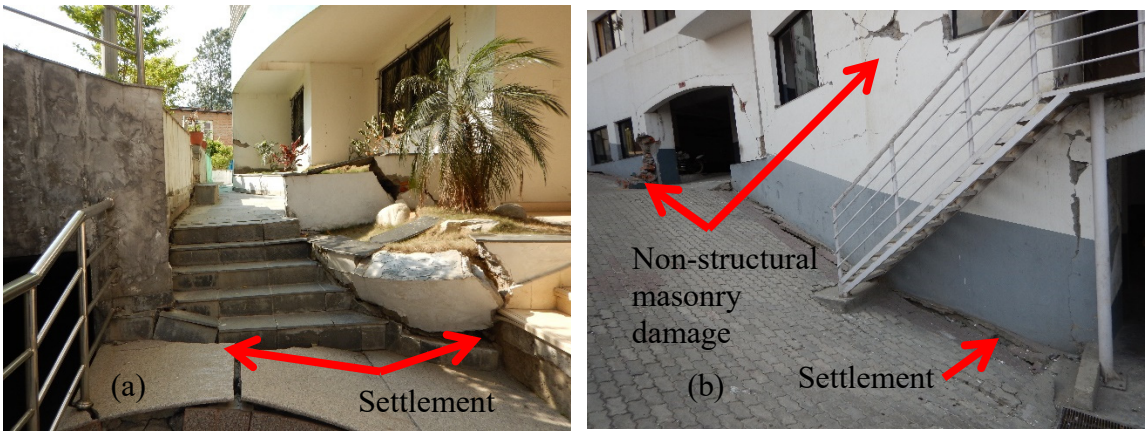

Figure 3.39 Swayambhu Apartment Complex – backfill settlement.

SUMMARY

Researchers from the University of Illinois at Urbana-Champaign – Youssef Hashash (in collaboration with a GEER Association team) and Larry Fahnestock – visited Nepal in late May and early June 2015 to study the geotechnical aspects and structural response of buildings related to the April 25, 2015 Gorkha Earthquake (M7.8) and its related aftershocks. Ground reconnaissance was conducted in and around Kathmandu, with several excursion to remote areas. Aerial reconnaissance was conducted to extensively explore geotechnical aspects in a wider range of remote areas.

4.1 Geotechnical aspects

The April 25, 2015, M7.8 Gorkha earthquake occurred in the actively deforming central Himalayan mountain range area approximately 80km northwest of Kathmandu, Nepal. This mainshock and the largest aftershock (May 12, 2015, M7.3) were both blind since they did not rupture the surface. The mainshock and related aftershocks triggered significant landsliding that killed hundreds of people, blocked several roads, buried villages, and dammed natural rivers. The Kathmandu Valley contains lake and river sediments that can deform due to either cyclic failure or liquefaction when shaken. Ground failures due to weak soils were almost exclusively in this region, and the weak soils that caused ground damage ranged from fine sands to silty sands to silty clays. At power plants outside Kathmandu, excessive settlement, landsliding and rockfalls were observed. Additional details on geotechnical aspects can be found in the GEER Report (Hashash et al. 2015).

4.2 Structural response of buildings

Three broad building classifications are used in Nepal: wood-framed construction, unreinforced load-bearing masonry (URM) wall construction and reinforced-concrete (RC) frame construction. All building types experienced damage and collapse as a result of the earthquake sequence. The investigation documented in this report focused on RC frame buildings, which exhibited a wide range of performance from minor damage to complete collapse. Additional observations related to RC frame buildings, as well as to wood-framed and URM buildings can be found in documentation from the EERI reconnaissance team (Lizundia et al. 2015).

Typical low-rise to mid-rise RC frame buildings suffered from a wide range of deficiencies that negatively impacted seismic performance. Chief amongst these is the lack of an enforced building code, and even simple rules of thumb established over two decades ago appear to be almost universally ignored. The range of deficiencies includes: poor material quality, no inspection or quality control, very light column reinforcement (longitudinal and transverse), no ductile detailing in beam-column joints and potential hinge regions, pervasive and severe geometric irregularities, buildings constructed beyond permitted height and heavy brick masonry infill. Masonry infill is not intended to be

structural, but it is built tight against the RC frame, and as a result, significantly affects structural earthquake response.

In Kathmandu, RC frame construction is used extensively for buildings with residential, commercial and combined residential / commercial function. These buildings are typically constructed by the owners in an ad hoc fashion with irregular structural layouts, using minimal steel reinforcement and whatever materials are available on site to mix concrete. Extensive non-ductile seismic response and collapse were observed for this class of building, with the Balaju region of Kathmandu hit particularly hard.

Although the majority of low-rise to mid-rise RC frame buildings in Kathmandu are owner-constructed with minimal formal planning, several mid-rise buildings visited were relatively new structures that had been more carefully developed, likely with some engineering input. These buildings typically had nonstructural damage and light to moderate structural damage.

In addition to being used extensively in residential / commercial buildings in Kathmandu, RC frame construction is also used in institutional buildings, such as government and university facilities. Since these buildings have more specific programmatic requirements as compared to the common residential / commercial sector, they typically have more regularity and have been more careful planned. Although they still had deficiencies and exhibited non-ductile response, the construction quality and detailing appear to be more similar to the developed residential / commercial buildings and better than the commonplace residential / commercial buildings.

Although low-rise construction has been dominant in Kathmandu for many years, mid-rise to high-rise construction (roughly 10 to 20 stories) has been used more recently for apartment buildings. These tall apartment buildings, largely opened within the past five years, are primarily RC frame structures, but they may also employ RC shear walls for lateral load resistance. Generally speaking, these mid-rise to high-rise buildings exhibited adequate structural performance during the earthquake sequence (no collapse and relatively modest structural damage), but they also experienced significant non-structural damage, including pounding. The primary structural systems of these buildings are proportioned, detailed and constructed according to more rigorous earthquake-resistant standards, but brick masonry is still used extensively for non-structural walls and architectural features, and this masonry was heavily damaged during the earthquake sequence, presenting a safety risk and necessitating major post-earthquake repair work.

Generally speaking, the structural response of buildings during the earthquake was problematic due to deficiencies. Many of these deficiencies can be mitigated reasonably with relatively simple proportioning and detailing requirements, along with construction quality control. Some of these requirements are already contained in official “rules of thumb” documents, and simply need to be respected in design and then enforced in the field. Establishing a more consistent and rigorous design and construction framework for buildings is critical in Nepal for preparedness to withstand future large earthquakes and to rebound rapidly after these future events.

REFERENCES

Chitrakar, G. and Pandey, M. (1986). "Historical Earthquakes of Nepal," Bulletin Geological Society of Nepal, 4, 7-8.

Collins, B.D., and Jibson, R.W. (2015). "Assessment of Existing and Potential Landslide Hazards Resulting from the April 25, 2015 Gorkha, Nepal Earthquake Sequence," U.S. Geological Survey Open-File Report 2015–1142, 50 p., dx.doi.org/10.3133/ofr20151142

Google (2016). DigitalGlobe Map data.

Hashash, Y., Tiwari, B., Moss, R., Asimaki, D., Clahan, K., Kieffer, D., Dreger, D., Macdonald, A., Madugo, C., Mason, H., Pehlivan, M., Rayamajhi, D. Acharya, I. and Adhikari, B. (2015). "Geotechnical Field Reconnaissance: Gorkha (Nepal) Earthquake of April 25, 2015 and Related Shaking Sequence," GEER Association Report No. GEER-040, Version 1.1, August 7, 2015, dx.doi.org/10.18118/G61591

Hyrdoworld (2015). http://www.hydroworld.com/articles/2015/05/nepal-s-456-mw-upper-tamakoshi-hydroelectric-project-suffers-settlement.html

KEC (2016). Kathmandu Engineering College, http://www.keckist.edu.np/keckist/contact (accessed March 1, 2016).

Lizundia, B., Shrestha, S., Bevington, J., Davidson, R., Jaiswal, K., Jimee, G., Kaushik, H., Kumar, H., Kupec, J., Mitrani-Reiser, J., Poland, C., Shreshta, S., Welton-Mitchell, C., Tremayne, H. and Ortiz, M. (2016) "EERI Earthquake Reconnaissance Team Report: M7.8 Gorkha, Nepal Earthquake on April 25, 2015 and its Aftershocks," EERI, May 2016.

Nepal (1994a). NBC 201: Mandatory Rules of Thumb for RC Frames with Masonry Infills, Gonvernment of Nepal, Ministry of Physical Planning and Works, Kathmandu, 1994.

Nepal (1994b). NBC 205: Mandatory Rules of Thumb for RC Frames without Masonry Infills, Gonvernment of Nepal, Ministry of Physical Planning and Works, Kathmandu, 1994.

Nepal (2015). *Nepal Earthquake 2015: Post Disaster Needs Assessment*, Government of Nepal, National Planning Commission, Kathmandu, 2015.

Ziselsberger, M. (2016). "Inventory of Earthquake-Induced Landslides in the Sindulpalchok District of Nepal Resulting from the M7.8 Gorkha Earthquakes and Related Aftershock Sequence. M.S. Thesis, Institute of Applied Geosciences, Graz University of Technology.

APPENDIX A: GPS COORDINATES FOR STRUCTURAL PHOTOGRAPHS

Table A.1 GPS coordinates for structural photographs.

Photo ID	Latitude (N)	Longitude (E)	Figure Label
DSCN0093	27,44',7.998"	85,18',18.918"	3.1a
DSCN0094	27,44',7.932"	85,18',18.87"	3.1b
DSCN0139	27,44',7.86"	85,18',29.058"	3.2a
DSCN0140	27,44',7.86"	85,18',29.058"	3.2b
DSCN0157	27,44',24.462"	85,18',50.196"	3.3
DSCN0167	27,44',20.226"	85,18',49.98"	3.4a
DSCN0173	27,44',21.282"	85,18',50.682"	3.4b
DSCN0160	27,44',21.744"	85,18',50.178"	3.5a
DSCN0165	27,44',21.846"	85,18',50.16"	3.5b
DSCN0162	27,44',21.828"	85,18',50.196"	3.5c
DSCN0148	27,44',24.51"	85,18',47.662"	3.6a
DSCN0152	27,44',24.516"	85,18',47.502"	3.6b
DSCN0069	27,38',19.596"	85,20',23.796"	3.7a
DSCN0062	27,38',19.86"	85,20',23.424"	3.7b
DSCN0063	27,38',20.4"	85,20',21.834"	3.7c
DSCN0061	27,38',19.896"	85,20',23.382"	3.7d
DSCN0579	27,41',53.766"	85,18',45.618"	3.8a
DSCN0569	27,41',52.32"	85,18',47.76"	3.8b
DSCN0563	27,41',52.536"	85,18',47.604"	3.9a
DSCN0552	27,41',51.714"	85,18',47.19"	3.9b
DSCN0539	27,41',51.834"	85,18',45.798"	3.10a
DSCN0541	27,41',51.858"	85,18',47.97"	3.10b
DSCN0517	27,41',52.746"	85,18',46.044"	3.11a
DSCN0521	27,41',52.686"	85,18',46.188"	3.11b
DSCN0346	27,40',45.204"	85,18',54.516"	3.12a
DSCN0344	27,40',46.806"	85,18',55.338"	3.12b
DSCN0338	27,40',45.468"	85,18',54.396"	3.13a
DSCN0336	27,40',45.432"	85,18',54.348"	3.13b
DSCN0137	27,44',6.69"	85,18',14.382"	3.14
DSCN0098	27,44',7.818"	85,18',13.032"	3.15a
DSCN0102	27,44',7.782"	85,18',12.63"	3.15b
DSCN0107	27,44',7.05"	85,18',11.844"	3.16a
DSCN0119	27,44',6.96"	85,18',11.574"	3.16b
DSCN0103	27,44',7.446"	85,18',11.97"	3.16c
DSCN0106	27,44',7.23"	85,18',11.814"	3.16d

Table A.1 GPS coordinates for structural photographs (continued).

Photo ID	Latitude (N)	Longitude (E)	Figure Label
DSCN0028	27,41',41.022"	85,19',7.488"	3.17a
DSCN0027	27,41',40.986"	85,19',6.972"	3.17b
DSCN0031	27,41',41.016"	85,19',7.02"	3.17c
DSCN0033	27,41',54.624"	85,17',47.778"	3.18
DSCN0036	27,41',55.092"	85,17',47.772"	3.19a
DSCN0038	27,41',55.18"	85,17',47.562"	3.19b
DSCN0042	27,41',54.84"	85,17',47.622"	3.20
DSCN0046	27,41',56.976"	85,17',50.184"	3.21
DSCN0047	27,41',55.812"	85,17',48.594"	3.22
DSCN0084	27,38',57.936"	85,19',56.844"	3.24a
DSCN0081	27,38',58.848"	85,19',55.998"	3.24b
DSCN0072	27,38',48.504"	85,20',9.366"	3.25a
DSCN0073	27,38',48.45"	85,20',9.576"	3.25b
DSCN0465	27,44',25.908"	85,19',29.226"	3.26a
DSCN0466	27,44',25.914"	85,19',29.196"	3.26b
DSCN0473	27,44',25.752"	85,19',28.38"	3.26c
DSCN0477	27,44',24.78"	85,19',27.798"	3.26d
DSCN0471	27,44',26.046"	85,19',28.422"	3.26e
DSCN0475	27,44',25.104"	85,19',28.026"	3.26f
DSCN0482	27,44',24.792"	85,19',27.012"	3.26g
DSCN0612	27,41',15.96"	85,19',36.228"	3.27
DSCN0369	27,42',14.706"	85,19',38.73"	3.29a
DSCN0391	27,42',14.91"	85,19',39.786"	3.29b
DSCN0423	27,42',15.162"	85,19',39.45"	3.29c
DSCN0583	27,42',14.592"	85,19',38.382"	3.29d
DSCN0404	27,42',15.372"	85,19',40.938"	3.30a
DSCN0405	27,42',15.45"	85,19',40.896"	3.30b
DSCN0371	27,42',15.018"	85,19',38.442"	3.31a
DSCN0372	27,42',14.88"	85,19',38.328"	3.31b
DSCN0598	27,42',15.348"	85,19',39.348"	3.32a
DSCN0596	27,42',15.006"	85,19',39.624"	3.32b
DSCN0595	27,42',15.258"	85,19',39.384"	3.32c
DSCN0399	27,42',15.18"	85,19',40.59"	3.32d
DSCN0376	27,42',14.928"	85,19",39.486"	3.33a
DSCN0379	27,42',14.958"	85,19',39.834"	3.33b
DSCN0381	27,42',14.958"	85,19',39.852"	3.33c

Table A.1 GPS coordinates for structural photographs (continued).

Photo ID	Latitude (N)	Longitude (E)	Figure Label
DSCN0240	27,41',31.824"	85,22',15.246"	3.35a
DSCN0246	27,41',31.866"	85,22',16.896"	3.35b
DSCN0238	27,41',31.146"	85,22',16.098"	3.36a
DSCN0241	27,41',30.132"	85,22',14.646"	3.36b
DSCN0202	27,42',35.298"	85,16',48.894"	3.37
DSCN0176	27,42',35.544"	85,16',49.092"	3.38a
DSCN0177	27,42',36.144"	85,16',49.326"	3.38b
DSCN0185	27,42',37.08"	85,16',49.146"	3.39a
DSCN0194	27,42',36.834"	85,16',49.824"	3.39b

List of Recent NSEL Reports

No.	*Authors*	*Title*	*Date*
030	Chang, C.-M. and Spencer, B.F.	Multi-axial Active Isolation for Seismic Protection of Buildings	May 2012
031	Phillips, B.M. and Spencer, B.F.	Model-Based Framework for Real-Time Dynamic Structural Performance Evaluation	August 2012
032	Moreu, F. and LaFave, J.M.	Current Research Topics: Railroad Bridges and Structural Engineering	October 2012
033	Linderman, L.E., Spencer, B.F.	Smart Wireless Control of Civil Structures	January 2014
034	Denavit, M.D. and Hajjar, J.F.	Characterization of Behavior of Steel-Concrete Composite Members and Frames with Applications for Design	July 2014
035	Jang, S. and Spencer, B.F.	Structural Health Monitoring for Bridge Structures using Wireless Smart Sensors	May 2015
036	Jo, H. and Spencer, B.F.	Multi-scale Structural Health Monitoring using Wireless Smart Sensors	May 2015
037	Li, J. and Spencer, B.F.	Monitoring, Modeling, and Hybrid Simulation: An Integrated Bayesian-based Approach to High-fidelity Fragility Analysis	May 2015
038	Sim, S-H. and Spencer, B.F.	Decentralized Identification and Multimetric Monitoring of Civil Infrastructure using Smart Sensors	June 2015
039	Giles, R.K. and Spencer, B.F.	Development of a Long-term, Multimetric Structural Health Monitoring System for a Historic Steel Truss Swing Bridge	June 2015
040	Spencer, B.F., Moreu, F. and Kim, R.E.	Campaign Monitoring of Railroad Bridges in High-Speed Rail Shared Corridors using Wireless Smart Sensors	June 2015
041	Moreu, F. and Spencer, B.F.	Framework for Consequence-based Management and Safety of Railroad Bridge Infrastructure Using Wireless Smart Sensors (WSS)	June 2015
042	Spencer, B.F. and Gardoni, P. (Eds.)	Innovations and Advances in Structural Engineering: Honoring the Career of Yozo Fujino	August 2015
043	Asai, T. and Spencer, B.F.	Structural Control Strategies for Earthquake Response Reduction of Buildings	August 2015
044	Kim, R. and Spencer, B.F.	Modeling and Monitoring of the Dynamic Response of Railroad Bridges using Wireless Smart Sensors	September 2015
045	Wierschem, N. and Spencer, B.F.	Targeted Energy Transfer using Nonlinear Energy Sinks for the Attenuation of Transient Loads on Building Structures	September 2015
046	Fahnestock, L.A. and Hashash, Y.M.A.	Structural and Geotechnical Observations after the April 25, 2015 M7.8 Gorkha, Nepal Earthquake and its Aftershocks	December 2016